

# **The elusive functions of EXT1 and EXT2**

**Osman Goni**



**Centre for International Health and Department of Biomedicine  
Faculty of Medicine  
University of Bergen, Norway  
2021**

# **The elusive functions of EXT1 and EXT2**

**Osman Goni**

This thesis is submitted in partial fulfilment of the requirements for the degree of Master of Philosophy in Global Health at the University of Bergen.

**Centre for International Health and Department of Biomedicine  
Faculty of Medicine  
University of Bergen, Norway  
2021**



## ABSTRACT

Many human diseases with a high disease burden worldwide such as for example different forms of cancer, infectious diseases and autoimmune diseases are affected by the polysaccharide Heparan Sulfate (HS). The actions of HS largely depend on the structure of its polysaccharide chains that provide specific binding sites for proteins.

The aim of this master project was to gain more understanding of how the biosynthesis of HS is regulated, focusing on the HS biosynthesis enzymes, exostosin (EXT)1 and EXT2. The EXT-proteins have a key role in generating the HS polysaccharide backbone composed of alternating glucuronic acid (GlcA) and N-acetylglucosamine (GlcNAc) units. It is suggested that the biologically functional unit in HS chain elongation is a Golgi-complex containing EXT1 and EXT2. Due to the low enzyme activities of EXT2 it has been speculated that EXT2 is not involved in the actual elongation of the HS backbone but serves as a transport protein to transport EXT1 from the endoplasmic reticulum to the Golgi apparatus where HS elongation takes place. This will mean that EXT1 alone is elongating HS. Still, there are some indications that EXT2 may have some, but low, elongating enzyme activity. However, this has been difficult to study as the EXT proteins tend to associate with each other and to remain associated also after purification. In this thesis, to be able to in detail study of individual enzyme activities of the EXT proteins, human cells lacking either EXT1 or EXT2 were transiently transfected with the full-length EXT2 plasmid and EXT1 plasmid DNA in EXT1 and EXT2 deficient cells, respectively.

In this study we found that when the EXT2 protein was expressed in mouse cells lacking EXT1, the expressed EXT2 transferred glucuronic acid to an acceptor oligosaccharide, indication that EXT2 has HS elongating activity. However, this result was not repeated when similar experiments were done in a human cell line lacking EXT1. Further studies are needed to determine the role of EXT2 on HS elongation.

## CONTENTS

<b>ABSTRACT</b> .....	<b>i</b>
<b>ABBREVIATIONS</b> .....	<b>iv</b>
<b>ACKNOWLEDGEMENTS</b> .....	<b>vi</b>
<b>1 INTRODUCTION</b> .....	<b>1</b>
1.1 Proteoglycans and glycosaminoglycans .....	1
1.2 Heparan sulfate/heparin proteoglycans .....	3
1.2.1 HSPGs associated with the cell surface .....	3
1.2.2 HSPGs found in the ECM .....	4
1.2.3 HSPGs found inside the cells .....	4
1.3 Functions of heparan sulfate proteoglycans .....	5
1.4 Biosynthesis of heparan sulfate .....	7
1.5 HS chain initiation and elongation .....	7
1.5.1 HS chain initiation .....	7
1.5.2 HS chain elongation/polymerization .....	8
1.5.3 HS chain modifications .....	8
1.6 THE EXT-FAMILY .....	10
1.6.1 EXT1 and EXT2 .....	10
1.6.2 EXTL1 .....	11
1.6.3 EXTL2 .....	11
1.6.4 EXTL3 .....	12
1.7 Exostosin proteins and hereditary multiple exostoses .....	12
<b>2 AIMS/OBJECTIVES</b> .....	<b>13</b>
<b>3 RELEVANCE TO GLOBAL HEALTH</b> .....	<b>14</b>
<b>4 MATERIALS</b> .....	<b>15</b>
<b>5 METHODS</b> .....	<b>19</b>
5.1 Cell culture .....	19
5.2 Cell splitting .....	19
5.3 Cell Freezing .....	19
5.4 Cell transfection .....	20
5.5 Protein expression analysis .....	20
5.6 Glycosyltransferase assays .....	20
5.7 Western blot analysis .....	21
5.7.1 BCA protein assay .....	21
5.7.2 SDS PAGE electrophoresis .....	22
5.8 Gel Chromatography .....	23
5.8.1 Gel column preparation .....	23

5.8.2	<i>Sephadex G-25 gel chromatography</i> .....	23
5.9	Gene expression analysis by RT-PCR.....	24
5.9.1	<i>RNA extraction</i> .....	24
5.9.2	<i>cDNA synthesis</i> .....	24
5.9.3	<i>Quantitative real Time-Polymerase chain reaction (RT-PCR)</i> .....	24
5.10	Immunofluorescence staining.....	25
5.10.1	<i>Cell plate preparation</i> .....	25
5.10.2	<i>Cell staining</i> .....	25
5.11	Metabolic labeling with <sup>3</sup> H-glucosamine and analysis of heparan sulfate structure .....	26
5.11.1	<i><sup>3</sup>H-glucosamine metabolic labeling</i> .....	26
5.11.2	<i>Alkali treatment to release O-linked oligo and polysaccharides from proteins</i> .....	26
5.11.3	<i>Isolate free chains on DEAE-Sephacel</i> .....	26
5.11.4	<i>Desalting using PD 10 Columns</i> .....	27
5.11.5	<i>Chondroitinase ABC digestion</i> .....	27
5.11.6	<i>Superose 6 HPLC gel filtration column</i> .....	28
<b>6</b>	<b>RESULTS</b> .....	<b>29</b>
6.1	EXT1 deficient (EXT1KO) B16F10 mouse melanoma cells transfected with tGFP tagged EXT2 plasmid DNA .....	29
6.1.1	<i>Protein expression analysis by Western blotting</i> .....	29
6.1.2	<i>EXT2 mRNA expression levels in WT control, EXT1KO control, WT+ EXT2 and EXT1KO+EXT2 B16F10 mouse melanoma cells</i> .....	30
6.1.3	<i>Glycosyltransferase activity in WT control, EXT1KO control and EXT1KO+EXT2 B16F10 mouse melanoma cells</i> .....	31
6.1.4	<i>Immunofluorescence staining</i> .....	33
6.2	EXT1 deficient MV3 human cells transfected with tGFP tagged EXT2 plasmid DNA .....	33
6.2.1	<i>Protein expression analysis by Western blotting</i> .....	34
6.2.2	<i>EXT2 mRNA expression levels in WT control, EXT1KO control, WT+ EXT2 and EXT1 KO+EXT2 MV3 human cells</i> .....	35
6.2.3	<i>Glycosyltransferase activity in WT control, EXT1KO control and EXT1 KO+EXT2 MV3 human cells</i> 36	36
6.3	EXT2 deficient B16F10 mouse melanoma transfected with full-length human C-terminal myc-DDK-tagged EXT1 plasmid DNA.....	36
6.3.1	<i>Protein expression analysis by Western blotting</i> .....	36
6.3.2	<i>EXT1 mRNA expression levels in WT control, EXT2KO control, WT+ EXT1 and EXT2KO+EXT1 B16F10 mouse melanoma cells</i> .....	37
6.3.3	<i>Glycosyltransferase activity in WT control, EXT2KO control and EXT2 KO+EXT1 B16F10 mouse melanoma cells</i> .....	38
<b>7</b>	<b>DISCUSSION</b> .....	<b>39</b>
<b>8</b>	<b>CONCLUSION</b> .....	<b>42</b>
<b>9</b>	<b>REFERENCES</b> .....	<b>43</b>

## ABBREVIATIONS

<b>HS</b>	Heparan sulfate
<b>CS</b>	Chondroitin sulfate
<b>PG</b>	Proteoglycan
<b>HSPG</b>	Heparan sulfate proteoglycan
<b>CSPG</b>	Chondroitin sulfate proteoglycan
<b>GAGs</b>	Glycosaminoglycans
<b>ECM</b>	Extracellular matrix
<b>EXT</b>	Exostosin
<b>EXTL</b>	Exostosin like
<b>EXT1KO</b>	Exostosin 1 Knock-out
<b>EXT2KO</b>	Exostosin 2 Knock-out
<b>WT</b>	Wild Type
<b>MO</b>	Multiple osteochondromas
<b>NDST</b>	N-deacetylase/N-sulfotransferase
<b>DMEM</b>	Dulbecco's modified Eagle's medium
<b>RPMI</b>	Roswell Park Memorial Institute
<b>PBS</b>	Phosphate buffered saline
<b>RT-PCR</b>	Real time polymerase chain reaction
<b>RNA</b>	Ribonucleic acid
<b>DNA</b>	Deoxyribonucleic acid
<b>cDNA</b>	Complementary Deoxyribonucleic acid
<b>HPRT</b>	Hypoxanthine-guanine phosphoribosyltransferase
<b>POLR2F</b>	Polymerase II Subunit F
<b>SDS</b>	Sodium dodecyl sulfate
<b>GAPDH</b>	Glyceraldehyde-3-phosphate dehydrogenase
<b>HRP</b>	Horse radish peroxidase
<b>ECL</b>	Enhanced chemiluminescence
<b>IgG</b>	Immunoglobulin G
<b>GlcA</b>	Glucuronic acid
<b>GlcNAc</b>	N-acetylglucosamine

<b>UDP</b>	Uridine diphosphate
<b>Myc</b>	myc tag, a polypeptide protein tag derived from the c-myc gene product
<b>tGFP</b>	turbo bright green fluorescent protein
<b>DEAE</b>	Diethylaminoethyl
<b>PFA</b>	Paraformaldehyde
<b>CPM</b>	Counts per minute



## ACKNOWLEDGEMENTS

First and foremost, all praises and gratitude to the Almighty, for His sprinkles of blessings throughout my research work to complete the research successfully during the Covid-19 pandemic.

I would like to express my wholehearted gratitude to my research supervisor, Prof. Marion Kusche-Gullberg, Department of Biomedicine, University of Bergen, Norway, for giving me the opportunity to conduct this research and providing inestimable guidance throughout the research. Her perseverance, vision, sincerity and motivation have inspired me. It was a tremendous privilege and honor to be a part of this research under her supervision. I am grateful to her for her continuous support in lab work and edifying lectures regarding the research project throughout the research. She has invested lots of her valuable time and always kept encouraging me till the last of my thesis. I am grateful to her for the enormous support to make me understand every step of the research and lab work. I have got a precious opportunity to work with her which has created a strong platform for me. I am extremely grateful to her for her friendly, empathetic and encouraging behavior throughout the research process that has helped me to complete the research.

I would like to thank Mona Helen Grønning for her immense technical support in the lab. I am extremely grateful to her because of her efforts what she has dedicated for me to complete all the lab works without making mistakes as much as possible. She has been assisting me as a shadow of mine while conducting experiments in the lab. Accomplishing my thesis would be very cumbersome without her assistance.

I would also like to extend my thanks to Prof. Donald Gullberg for his valuable guidance during the laboratory sessions regarding my thesis that helped me to a lot utilizing the thesis ideas. I am also thankful to all members of Matrix Biology family for supporting me all the way through my research.

I am very much grateful to my family members for their constant support, love and prayers to complete my thesis.

Osman Goni.  
University of Bergen, Norway.  
May 2021.

# 1 INTRODUCTION

Heparan sulfate (HS) is a sulfated polysaccharide that is bound to different proteins to form heparan sulfate proteoglycans (HSPGs). HSPGs are found at cell surfaces and in the extracellular matrix (ECM). HS is similar to the polysaccharide heparin but in contrast to heparin, that is only found inside mast cells but HS is made by all cells in the body. Heparin is used in the clinics as an anticoagulant since 1935s (Rabenstein, 2002). However, the physiological role of heparin in the mammalian body is unclear but its function is probably related to storage of proteases in connective tissue mast cell granules (Mulloy et al., 2017). Heparin chains are uniformly sulfated whereas HS has a more varied structure, composed of sulfated and non-sulfated domains. HSPGs play important roles in several physiological and pathological processes, including normal fetal development, wound healing, inflammation, microbial infections and cancer progression. (Bishop et al., 2007)(Li & Kusche-Gullberg, 2016).

The biological activities depend on the ability of HS to bind proteins in a selective fashion. Some mouse models with defects in enzymes involved in HS biosynthesis are embryonic lethal whereas others show different abnormalities including formation of bone tumors, abnormal skeletal and kidney development and eye defects. Mutations caused by disturbed HS synthesis in humans are mostly autosomal dominant inherited disorders, often with overlapping phenotypic features, characterized by growth disorders and skeletal deformities or are linked to neurologic disorders (Li & Kusche-Gullberg, 2016). There has been a lot of studies on the biosynthesis of HS and how the large structural variation of HS contributes its ability to bind other molecules and thus influence both physiological and pathological events. However, the regulation of HS biosynthetic machinery that generates cell specific HS structures, is still poorly understood.

## 1.1 Proteoglycans and glycosaminoglycans

Proteoglycans (PGs) are glycoproteins composed of a core protein with one or more covalently attached polysaccharide chains called glycosaminoglycans (GAGs)(Li & Kusche-Gullberg, 2016) (Fig.1).

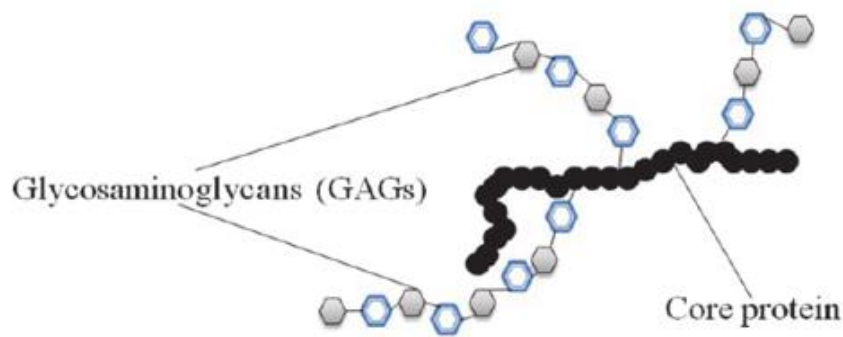


**Fig. 1: Schematic figure of a proteoglycan molecule containing a core protein with attached glycosaminoglycan chains** (Marie et al., 2011).

GAGs are long unbranched polysaccharide chains consisting of a backbone of repeating disaccharide units composed of a hexuronic acid (glucuronic acid, GlcA or iduronic acid, IdoA) or a galactose (Gal) and a hexosamine (N-acetylglucosamine, GlcNAc or N-acetylgalactosamine, GalNAc) residues. Most GAG chains are sulfated to a variable extent, which allows a large degree of structural variation. Based on the nature and sulfation level of the repeated disaccharide, GAGs can be divided into several classes: heparan sulfate (HS), heparin (a highly sulfated variant of HS), chondroitin sulfate (CS), dermatan sulfate, keratan sulfate and hyaluronan (Kristian Prydz, 2015). The repeating disaccharide in HS and heparin is GlcA/IdoA-GlcNAc and in CS GlcA-GalNAc. Dermatan sulfate (GlcA/IdoA-GalNAc) is similar to CS but in dermatan sulfate some GlcA residues have been epimerized to IdoA. In keratan sulfate the hexuronic acid has been replaced by a galactose and keratan sulfate is built up of alternating galactose (Gal) and GlcNAc residues (Kusche-Gullberg & Kjellén, 2003). Hyaluronan is composed of repeating GlcA-GlcNAc disaccharide units and, in contrast to the other GAGs, it is not linked to a core protein and is not sulfated (Fig. 2). When different types of GAG-chains are attached to the same core protein it is called a hybrid PG (Noborn et al., 2016). The sulfated polysaccharide chains are highly negatively charged molecules. The modification of GAG chains by sulfation at different site contribute to their ability to bind to and modulate the activity of a multitude of ligands thus influencing biological processes, from patterning and organogenesis in the early embryo to adult homeostasis and ageing (Kramer, 2010). This thesis will mostly deal with HS focusing on its biosynthesis, functions and the EXT proteins.

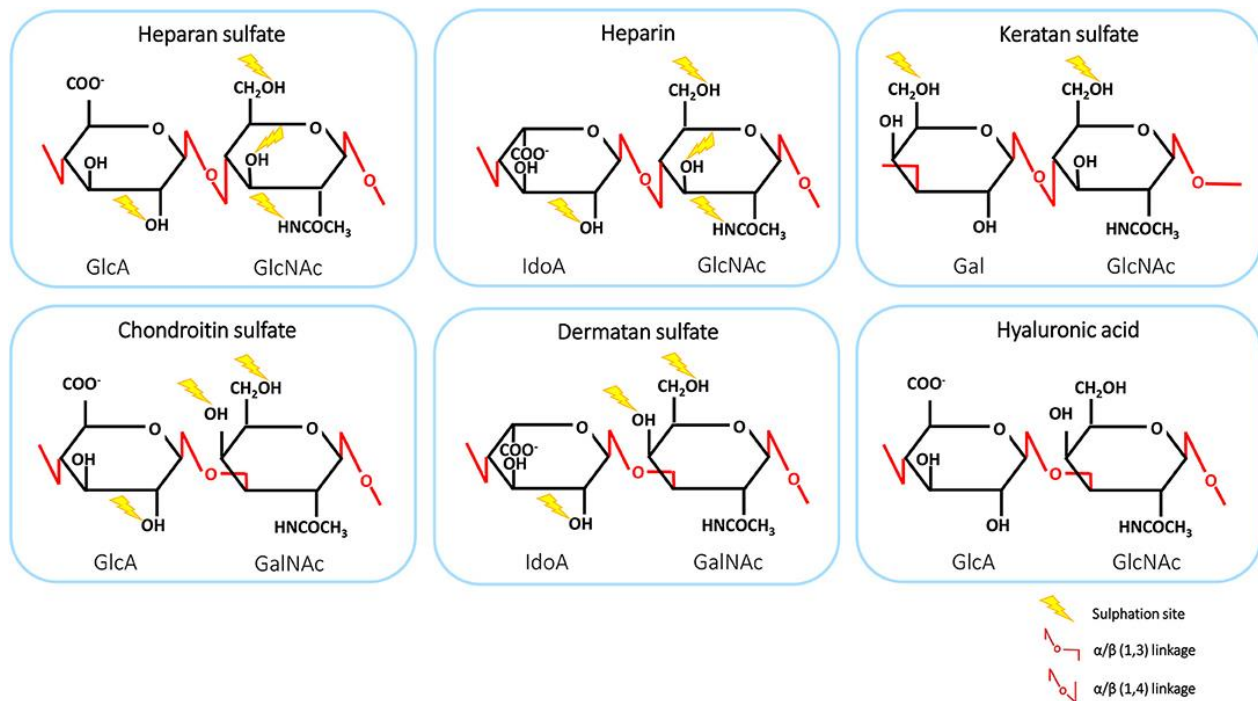


**Fig. 2: The structure and disaccharide composition of glycosaminoglycans (GAGs).** The backbone of GAGs consists of repeating disaccharide subunits, composed of uronic acid or galactose and an amino sugar. Linkages are shown in red and sites of sulphation are indicated by yellow lightning bolts. GlcA, D-glucuronic acid; GlcNAc, N-acetyl-D-glucosamine; GalNAc, N-acetyl-D-galactosamine; Gal, D-galactose; IdoA, L-iduronic acid. Figure from (Crijs et al., 2020).

## 1.2 Heparan sulfate/heparin proteoglycans

Heparan sulfate proteoglycans (HSPGs) are major components of the ECM and ubiquitously present on the cell surface (Li & Kusche-Gullberg, 2016). HSPGs can be classified after the sugar composition of their GAG chains as described above. However, it is more common to classify HSPGs according to their cellular localization: associated with the cell membrane, in the ECM or inside the cell.

### 1.2.1 HSPGs associated with the cell surface

The two main families of cell surface HSPGs are syndecans and glypicans. The cell surface HSPGs can modulate a number of cellular events like cell-cell and cell-matrix interaction, cellular signaling and internalization of ligands. Syndecans are transmembrane proteins containing HS or both

HS and CS chains. In humans, there are four syndecans: syndecan-1-4. Syndecan-2 and syndecan-4 carry only HS chains whereas syndecan-1 and syndecan-3 can have both HS and CS chains.

Glypicans are attached to the cell membrane by a glycosyl-phosphatidylinositol (GPI) anchor. The human glypican family has 6 members, glypican 1-6, that all have HS chains. Another characteristic for all glypicans is that the HS chains are located close to the plasma membrane (Hull et al., 2017)

### 1.2.2 *HSPGs found in the ECM*

Perlecan, collagen XVIII, and agrin are HSPGs found in the basement membrane, a network of ECM proteins found on the basolateral membrane of epithelial and endothelial cells around other cell types, such as muscle, Schwann and fat cells. These PGs are connected to other ECM molecules such as for example, fibronectin and collagens. By acting as cross-linkers of different ECM components, they provide support for cells. They have many different functions in development and wound healing that depend on both the core proteins and the GAG chains.

Perlecan is expressed by vascular smooth muscle cells and endothelial cells and released into the basement membrane (Annaval et al., 2020). Perlecan is a one of the largest monomeric matrix molecules. With GAG chains perlecan has a Mw of more than 750 kDa (the core protein is approximately 500 kDa and can be modified by the addition of 3-4 HS-chains and rarely one CS chain, approximately 65 kDa each) (Kallunki & Tryggvason, 1992)

Agrin is also a large ECM PG that is widely expressed in basement membranes and is important for the development of the neuromuscular junctions during embryogenesis.

Collagen XVIII has structural properties of both triple helical collagen and a HSPG. Proteolytic cleavage of the C-terminus of collagen type XVIII releases a domain called endostatin, that can reduce the vascular growth in tumors(Hull et al., 2017).

### 1.2.3 *HSPGs found inside the cells*

Serglycin is the only known PG in this class. Serglycin is found in secretory granules of hematopoietic cells and carry heparin and/or CS chains. Serglycin got its name because of its characteristic, extensive region of Ser-Gly repeats in the core protein. In connective tissue mast cells, the GAG is heparin whereas in other hematopoietic cells serglycin carry CS chains. This PG

has crucial role in granular storage of mediator related to inflammatory signals (Kolset & Pejler, 2011).

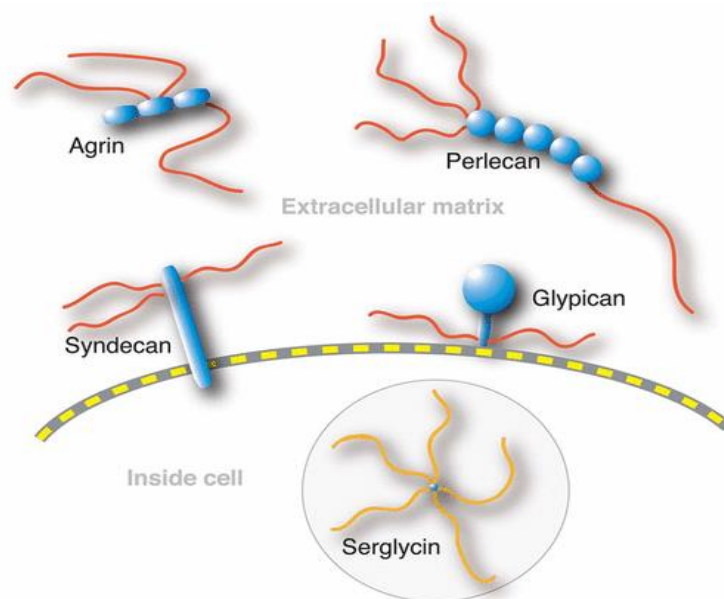


**Fig. 3. This figure illustrates different HSPG according to location.** Syndecan and glypican are present on the cell membrane, perlecan and agrin are found in the ECM and serglycin in mast cell granules. Figure from (Filipek-Górniok et al., 2021).

### 1.3 Functions of heparan sulfate proteoglycans

HSPGs are involved in both physiological and pathological processes throughout embryonic development, adult life and ageing. HSPGs interact with myriad of different proteins, such as proteases and their inhibitors, growth factors and morphogens, chemokines and adhesion proteins and can therefore mediate and regulate various cellular events (Bishop et al., 2007)(Gallagher, 2015) (Fig. 4). Depending on the molecules, the activity of the bound factors is either enhanced or inhibited by the binding to HS. The role of HSPGs in cell-signaling is an extensively studied field. HSPGs serve as co-receptors for growth factors and mediate their efficiency of binding to the receptor and causes activation of their high affinity receptors (Gallagher, 2015). Many signaling molecules such as for example fibroblast growth factors (FGFs), Wingless (Wnt/Wg), hedgehog (Hh), transforming growth factor-beta (TGF-beta) and bone morphogenic protein (BMP) need binding to HSPGs for proper function (Häcker et al., 2005).

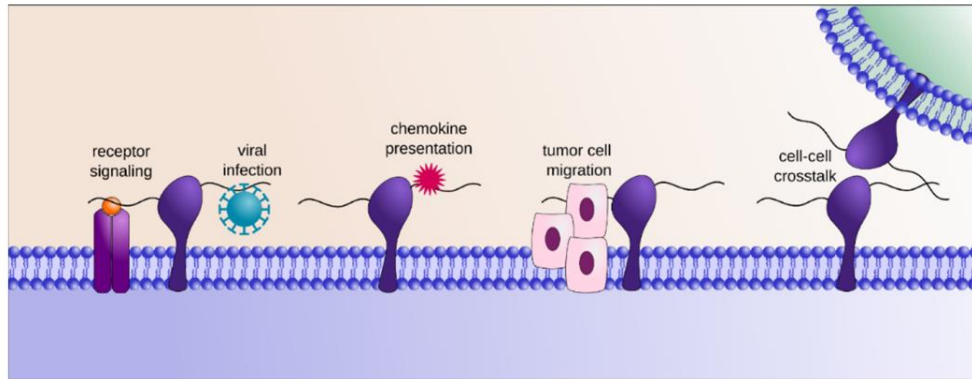


**Fig. 4: Different functions of HSPGs.** Heparan sulfate proteoglycans (HSPGs) contribute to the formation of the glycocalyx at the cell surface and are ubiquitously present in the extracellular matrix, where they interact with a myriad of different HS binding proteins. In doing so, they integrate the flow of information that circulates in-between cells and upstream signaling that is mediated by the cytokines/growth factors-receptor interaction. They are also further involved in chemokines/morphogens gradient stabilization and presentation, cell migration and adhesion or microbial adsorption, thereby regulating many fundamental biological processes. Figure from (Annavaal et al., 2020).

Pathogens, like many viruses (including herpes simplex virus, zika virus, HIV-virus and Covid-19-virus), parasites (like *Trypanosoma cruzi*), and bacteria (like *leptospira*, *N. gonorrhoeae*) bind to HS on the cell surface. This helps the pathogen to bind its cell surface protein receptor on the cell membrane and leads to internalization of the pathogen (Cagno et al., 2019)(Clausen et al., 2020).

The biological activities of HS largely depend on the location of sulfate groups on the polysaccharide chain that provide binding sites for myriad of proteins. Also, the number and length of the HS chains control the biological activities of HS. Some molecules, like the plasma protease inhibitor antithrombin and FGF2, bind to specific sulfation patterns (Fig. 5B) (van den Born et al., 1995)(Forsberg & Kjellén, 2001). Other molecules bind non-specifically to negative regions in HS. The structure of HSPG is cell and tissue-specific and change during development, with age and disease. More than one type of core protein can occur on the same cell type, but it is generally believed that the structure of the HS chain is cell specific. Consequently, HS chains from specific cell type have the same type of structure irrespective of core protein. Although both the core protein and the polysaccharide chain are important for the function of HSPGs, mutations in genes for various core proteins give generally (but not always) milder phenotypic change than lack of various enzymes that are involved in HS biosynthesis (Forsberg & Kjellén, 2001). This is most probably

due to that most cells synthesize several types of HSPGs and thus HS chains will still be present on the cells even when one species of core protein is missing.

## 1.4 Biosynthesis of heparan sulfate

Like DNA, RNA and protein synthesis, the formation of HS structure is not template driven. Instead, it depends on the organization and substrate specificity of the enzymes (approx. 25 different enzymes), the amount of precursor molecules (UDP-sugars and sulfate donor) and the rate of flow through the Golgi apparatus. The enzymes involved in HS synthesis are glycosyltransferases which build the HS backbone and modification enzymes, sulfotransferases and epimerases, that modify the sugars residues in patterns characteristic for each cell-type. The glycosyltransferases transfer activated sugars (UDP-sugars) to generate the HS polysaccharide backbone. The sulfate groups that will be incorporated into the growing chain by sulfotransferases must be activated before the sulfation reaction. In mammals, the activated form of the sulfate is the sulfonucleotide 3-phosphoadenosine 5-phosphosulfate (PAPS). The core proteins and enzymes involved in HS biosynthesis are formed in the rough endoplasmic reticulum (ER) and are transported to the Golgi compartment where HS chain formation occur (K. Prydz & Dalen, 2000) (Li & Kusche-Gullberg, 2016).

## 1.5 HS chain initiation and elongation

### 1.5.1 *HS chain initiation*

HS and CS chain formation is initiated by the formation of a tetrasaccharide called the GAG-protein linkage region. It is formed by addition of xylose to a serin residue in a serin-glycine sequence in the core protein by xylosyltransferase (Xyl) 1 or 2. Then two galactose residues are added by galactosyltransferase (GalT)-I and II, respectively. Finally, the last sugar in the HS- and CS-protein linkage region, a GlcA, is added by glucuronyltransferase (GlcAT) -I. During biosynthesis of both HS and CS the GAG-linker tetrasaccharide is modified by phosphorylation of the xylose residue which is necessary for elongation by stimulating galactosyltransferase II activity (Wen et al., 2014). The two galactose residues can be sulfated but this has only been observed for CSPG linker regions (de Waard et al., 1992). Addition of a fifth sugar unit determines if CS or HS chains will be synthesized on the core protein. Addition of a GalNAc residue results in synthesis of CS/dermatan



sulfate, while the transfer of a GlcNAc unit to the tetrasaccharide linkage region initiates HS synthesis (Li & Kusche-Gullberg, 2016).

### 1.5.2 *HS chain elongation/polymerization*

Elongation of HS chain is initiated by the addition of a GlcNAc unit to the linker region by exostosin-like 3. Then an enzyme complex of exostosin proteins EXT1 and EXT2 elongates HS chains by the alternating addition of GlcA and GlcNAc residues (Busse et al., 2007). The “stop signal” for chain elongation is not known and HS chains typically contain between 50–200 disaccharides.

### 1.5.3 *HS chain modifications*

During HS elongation HS chains are modified in a sequential process involving: 1) partial N-deacetylation/N-sulfation of GlcNAc units, 2) C5-epimerization of some GlcA to IdoA residues and, finally, 3) incorporation of O-sulfate groups at various positions (Fig. 5A).

N-deacetylation/N-sulfation is catalyzed by glucosaminyl *N*-Deacetylase/*N*-Sulfotransferases (NDSTs) that remove *N*-acetyl group from GlcNAc units and replace them with sulfate groups to form *N*-sulfated glucosamine units (GlcNS). NDST family has four family members, NDST-1, NDST-2, NDST-3 and NDST-4. The modifications by the NDST-enzymes occur in a block-wise fashion generating *N*-sulfated regions with GlcNS units and *N*-acetylated regions with GlcNAc residues. Due to the substrate specificity of the other modifying enzymes further modifications of the HS chains occur in or in the surrounding area of the *N*-sulfated regions (Ledin et al., 2004).

The C-5 epimerase enzyme converts GlcA to IdoA. There is only one isoform of the C-5 epimerase. This enzyme has immense role in HS flexibility. Epimerization in HS chain makes the chains flexible which promotes the interactions with different proteins involved in for example cell signaling and cellular communication (Qin et al., 2015).

Heparan sulfate 2-O sulfotransferase enzyme (only one isoform) is involved in transferring of sulfate groups to C2 position of IdoA and more rarely to GlcA. Sulfated IdoA residues play important roles in many HS-protein interactions like binding to different growth factors (Bethea et al., 2008).

Heparan sulfate 6-O sulfotransferase enzymes (three isoforms) transfer sulfate group to C6 position of GlcNS and GlcNAc units. 6-O sulfation of HS chain is important for many cellular processes such as HS binding to for example vascular endothelial growth factor and members of the FGF family (Nagai & Kimata, 2014).

Heparan sulfate 3-O-sulfation is a late and rare modification of HS chains. HS-3-O sulfotransferases add one sulfate group at C3 position of glucosamine units in HS chains. There are 7 family members (HS-3-OST-1, -2, -3A, -3B, -4, -5 and -6). HS-3-OST-1 and -5 isoforms create HS with high affinity for antithrombin (that is mediating the anticoagulation activity of heparin) and herpes simplex virus 1 glycoprotein D of Type I herpes simplex virus (essential for viral invasion of the target cell) (Chen et al., 2003).

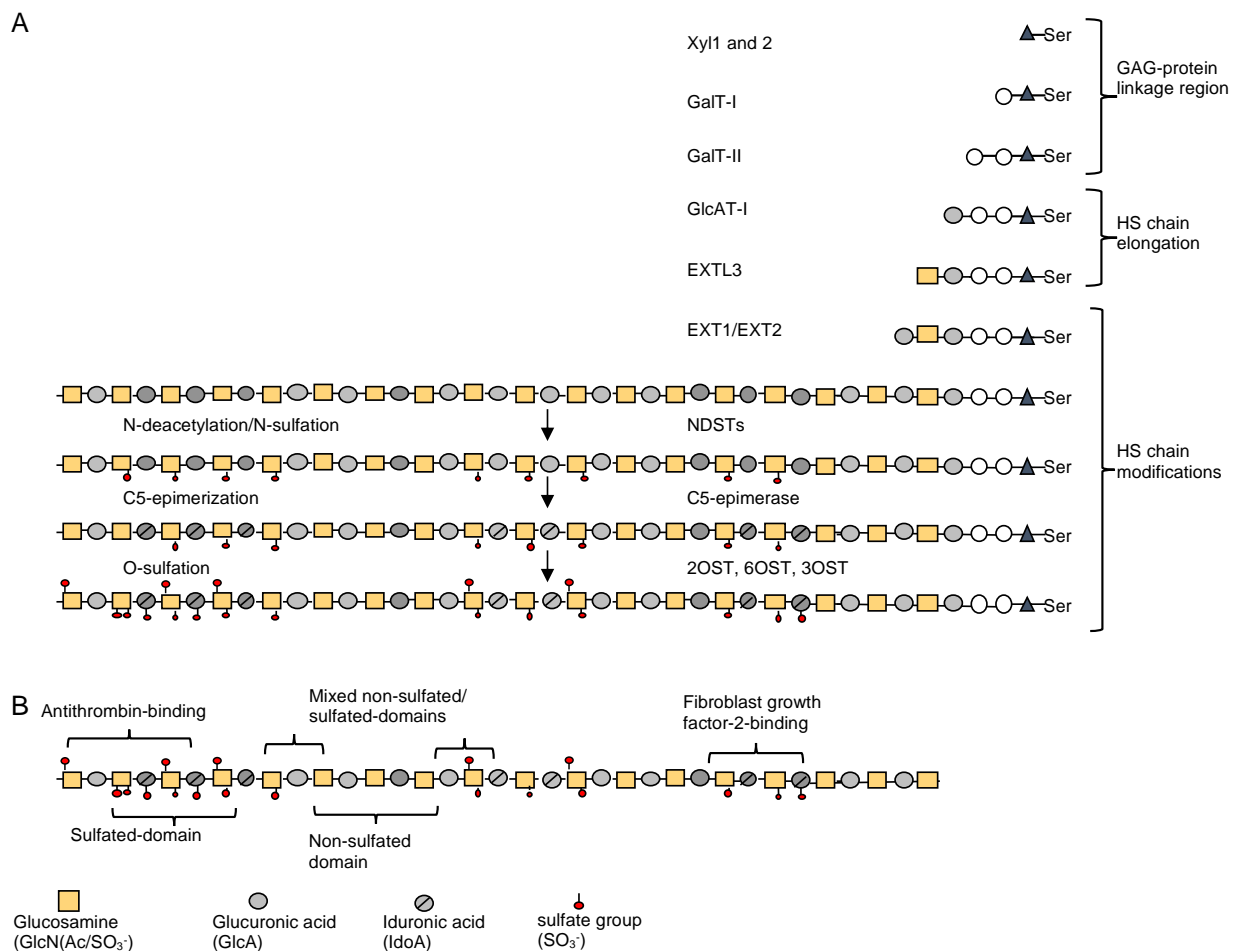


**Fig 5: Schematic illustration of HS biosynthesis.** A. Synthesis of the GAG-protein tetrasaccharide linker region by addition of xylose, two galactose residues and a GlcA to a serine residue on the core. After addition of a GlcNAc, elongation takes place by the alternating addition of GlcA and GlcNAc by EXT1/2. Modification starts with N-deacetylation/N-sulfation of a subset of GlcNAc, forming GlcNS. This modification is necessary for further

epimerization by the C5-epimerase and sulfations by 2-O-, 3-O- and 6-O-sulfotransferases (-OSTs). **B.** Typical for HS is that not all potential sites are modified and that the modifications tend to be clustered. This results in the creation of different domains along HS chains, sulfated, non/sulfated and mixed sulfated/nonsulfated domains. Shown are also the binding sites for antithrombin and fibroblast growth factor 2. Figure provided by Prof. M. Kusche-Gullberg.

## 1.6 THE EXT-FAMILY

The human exostosin (EXT)-family consists of five members; EXT1, EXT2 and three EXT-Like proteins, EXTL1, EXTL2 and EXTL3 (Busse-Wicher et al., 2014). EXT1 and EXT2 were first associated with the skeletal disorder Hereditary Multiple Exostoses, HME (describe below in EXOSTOSIN PROTEINS AND HEREDITARY MULTIPLE EXOSTOSES), hence the name exostosins. Based on *in vitro* enzyme activities, all 5 family members are proposed to take part in HS biosynthesis (Fig. 6). However, only EXT1, EXT2 and EXTL3 have been shown to be necessary for HS chain elongation (Busse & Kusche-Gullberg, 2003).

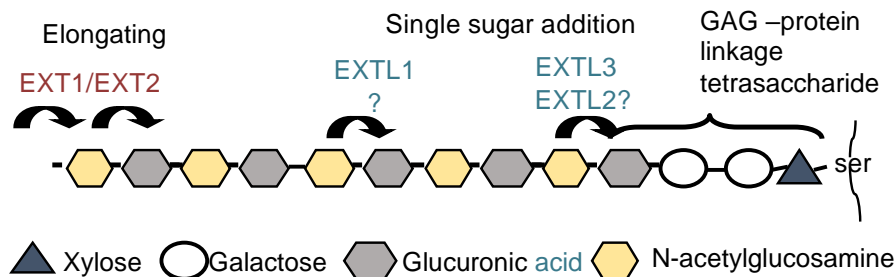


**Fig. 6: EXT-proteins and their proposed roles in HS chain-elongation.** A complex of EXT1 and EXT2 elongates the chain. EXTL3 initiates HS chains on a protein linkage tetrasaccharide. The roles of the EXTL1 and EXTL2 are unclear. Figure provided by Prof. M. Kusche-Gullberg.

### 1.6.1 *EXT1 and EXT2*

Elongation of HS chains is believed to occur by alternating addition of GlcA and GlcNAc, from their respective UDP-sugars, by a complex of EXT1 and EXT2. They are type II transmembrane protein located in the Golgi with an N-terminal cytoplasmic tail, a transmembrane domain, and a large globular domain containing the enzymatic activity (Mccormick et al., 2000) (Fig. 7). *In vitro*, EXT1 alone has both GlcNAc-transferase and GlcA-transferase activity and can elongating HS chain without EXT2 (Busse & Kusche-Gullberg, 2003). The function of EXT2 is unexplained. After overexpression of EXT2 in mammalian cells no enhanced glycosyltransferase enzymatic

activities was observed (Busse-Wicher et al., 2014). In contrast, siRNA silencing of either EXT2 or EXT1 had similar effects on HS chain length, they become shorter (Busse et al., 2007). Knock-out mice lacking EXT1 or EXT2 have the same phenotype. They lack HS chains and die during early embryonic development (Stickens et al., 2005). Thus, EXT2 clearly influences the catalytic activities of EXT1 and HS chain elongation. Studies have shown that EXT2 not only form a complex with EXT1 but also with NDST-1 and that NDST1 and EXT1 may compete for binding to EXT2 (Presto et al., 2008).

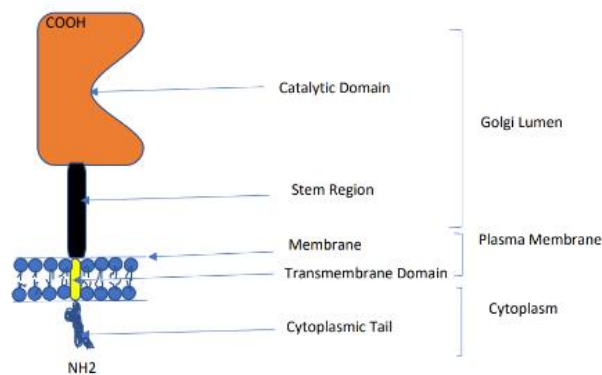


**Fig. 7: Schematic figure of a type II transmembrane protein.** The EXT family members are type II transmembrane protein located in the Golgi with an N-terminal cytoplasmic tail, a transmembrane domain, and a large globular domain containing the enzymatic activity (McCormick et al., 2000).

### 1.6.2 *EXTL1*

EXTL1 can transfer one single GlcNAc to oligosaccharides mimicking the growing HS chains *in vitro* (Kim et al., 2001). EXTL1 exists in all mammals but absent in lower vertebrates. In humans, the EXTL1 expression seems to be restricted to a few tissues such as the brain, liver and kidneys and skeletal muscles (Wise et al., 1997). As HS is synthesized by all cells in the body and as EXTL1 has a very restricted tissue expression EXTL1 does not seem to be necessary for or involved in HS biosynthesis. So far there is no publication of any model organism lacking EXTL1.

### 1.6.3 *EXTL2*

EXTL2 is also present in all mammals but not in the lower vertebrates. EXTL2 is expressed in all human tissues and has two *in vitro* glycosyltransferase activities, transfer of GlcNAc and GalNAc units to the GAG-protein linkage tetrasaccharide (Busse-Wicher et al., 2014). EXTL2 knock out

mice produce large amounts of GAG chains indicating that *in vivo*, EXTL2 might have a role in HS chain termination (Katta et al., 2015).

#### 1.6.4 *EXTL3*

*EXTL3* is expressed in all human tissues in both embryonic and adult lives and in all investigated species. *EXTL3* has two *in vitro* glycosyltransferase activities, transfer of GlcNAc residues involved in initiation and elongation of HS chains. *In vivo*, *EXTL3* appears only to be involved in the initiation of HS chains by adding of the first GlcNAc to the GAG-protein-linkage tetrasaccharide (Busse et al., 2007). Similar to mice lacking *EXT1* or *EXT2*, *EXTL3* KO mice die during early embryonic development and lack HS. (Takahashi et al., 2009).

### 1.7 Exostosin proteins and hereditary multiple exostoses

The name exostosin comes from the name used to describe the inherited bone disorder, hereditary multiple exostoses or osteochondromas (HME/MO), characterized by bony outgrowths around the growth plates in ribs, pelvis vertebrae and the long bones. The genes responsible for causing HME/MO were discovered by gene sequencing of affected patients (Stickens et al., 1996). The genes were named exostosin 1 (*EXT1*) and exostosin 2 (*EXT2*). Later it was found that these genes were involved in HS elongation (Lind et al., 1998). HME/MO is an autosomal dominant benign tumor characterized by multiple cartilage capped bony outgrowths (osteochondromas), which in a few cases (2 % of MO patients) is further transformed into chondrosarcoma or osteosarcomas. Incidence ratio of MO in population is about 1 per 50,000 live births. The exostoses give rise to chronic pain, limb deformities and neurological problems. The patients are heterozygote for the mutation and several different mutations in *EXT1* and *EXT2* have been reported in HME patients. The mutations are predominantly found in exons and randomly distributed over the entire *EXT1* gene, whereas *EXT2* mutations are more commonly found towards the N-terminal part of the protein (Pacifci, 2017). The *EXTL* proteins belong to the *EXT*-family based on amino acid sequence homology with *EXT1* and *EXT2* but are not associated with HME/MO (Busse-Wicher et al., 2014).

## 2 AIMS/OBJECTIVES

EXT1 and EXT2 proteins play major roles in HS chain biosynthesis. The specific focus of this study was to investigate the individual roles of EXT1 and EXT2 in HS elongation. It is suggested that EXT1 and EXT2 form a co-polymerase complex that elongates HS but the individual role of the two proteins in HS biosynthesis is not known. Deletion of either EXT1 or EXT2 in mice and human cells have shown that both proteins are necessary for HS chain elongation. Previous *in vitro* data shows that EXT1 has high enzyme activities related to HS elongation whereas the enzyme activities of EXT2 are very weak. Previously, it has been difficult to pinpoint the individual activities of EXT1 and EXT2 as the EXT proteins tend to associate with each other and to remain associated also after purification of recombinant proteins. The generation of cells lacking EXT1 or EXT2 has made it possible to study the individual activities of EXT1 and EXT2 by expressing EXT1 in a cell lacking EXT2 and EXT2 in a cell lacking EXT1.

*Overall Aim of this study:*

To clarify the role of EXT2; is it a glycosyltransferase or a chaperon?

Specific aims:

1. To determine transferase activities of EXT2 protein
2. To determine transferase activities of EXT1 protein

### 3 RELEVANCE TO GLOBAL HEALTH

The interactions of HSPGs with different protein ligands clearly influence global health. By interacting with growth factors and other signaling molecules, HS controls processes in pathogenesis of many disorders world wide including, inflammatory diseases, eye diseases, cancer, viral and bacterial infections (Lindahl & Kjellén, 2013). This has a significant impact when considering the high burden of these diseases world-wide. The key to understand the function of EXTs and HS in disease is to clarify how they are regulated in normal physiology. The results from this project will help us to better understand how EXT protein interactions are regulated and HS chain length determined in normal cells. This knowledge is essential for our understanding of what is changed in HS structure in disease.

## 4 MATERIALS

**Table 1. Cell lines**

Cell line	Provided by
EXT1KO B16F10 mouse melanoma cell (P 16)	Dr. Christian Gorzelanny, PhD University Hospital Hamburg-Eppendorf Department of Dermatology Germany
EXT2KO B16F10 mouse melanoma cell	
WT B16F10 mouse melanoma cell (P 39)	
EXT1KO MV3 human cell (P 3)	
WT MV3 human cell	

**Table 2. Cell culture reagents and materials**

Reagent	Supplier	Cat. no/Ref. no
Dulbecco's modified eagle medium (DMEM) GlutaMAX	Gibco	Ref: 31966-021
Fetal bovine serum (FBS)	Corning	Ref: 35-015-CV
Antibiotic-Antimycotic (AA)	Gibco	Ref: 15240-062
Dulbecco's phosphate buffered saline (PBS)	Sigma-Aldrich	Cat no: D8537
0.05% Trypsin-EDTA	Sigma-Aldrich	Ref: 25300-054
Dimethyl Sulfoxide (DMSO)	Sigma-Aldrich	Cat no: D2660
RPMI-1640 medium with 25mM HEPES without L-glutamine.	Sigma-Aldrich	Cat no: R5886
Cell culture flasks (25 and 75 cm <sup>2</sup> )	Thermo Scientific	Cat.no: 156367 & 156499
Nunclon Cell culture dishes (25 cm <sup>2</sup> )	Thermo Scientific	Cat.no: 150288

**Table 3. Transfecting agents**

Name	Supplier	Cat. no/Ref. no
Human tGFP-tagged EXT2 (NM_207122) plasmid DNA	Origene	Cat. no: RG204067
Human Myc-DDK-tagged EXT1 (NM_000127) plasmid DNA	Origene	Cat. no: RC200644
Lipofectamin 2000 transfection reagent	Invitrogen	Ref: 11668-027



**Table 4. Chemicals and materials for transferase assays and BCA protein assay**

Reagent	Supplier	Cat. no/Ref. no
Buffer mix (4.25 $\mu$ l/25 $\mu$ l assay)	0.2 M MgCl <sub>2</sub> , 0.1 M CaCl <sub>2</sub> , 2 M NaCl, 1 M HEPES pH 7.4 and freshly prepared	
GlcNAc[GlcA-GlcNAc] <sub>n</sub> GlcA acceptor substrates [GlcA-GlcNAc] <sub>n</sub> GlcNAc acceptor substrates	Made from <i>Escherichia coli</i> K5 capsular polysaccharide in the lab of M. Kusche-Gullberg	
UDP-[ <sup>3</sup> H]GlcNAc (100:1 ratio labeled and unlabeled UDP-GlcNAc, final conc. of UDP [ <sup>3</sup> H]GlcNAc, 0.1 $\mu$ Ci/ $\mu$ l)	PerkinElmer	Ref: NET434050UC
UDP-[ <sup>14</sup> C]GlcA (100:1 ratio labeled and unlabeled UDP-GlcA, final conc. of UDP-[ <sup>14</sup> C]GlcA, 0.02 $\mu$ Ci/ $\mu$ l).	PerkinElmer	Ref: NEC414050UC
Price BCA Protein Assay Kit	Thermo Scientific	Ref no: 23225

**Table 5. Antibodies**

Primary antibody	Supplier	Cat. no/Ref. no
Mouse monoclonal anti-turboGFP antibody	Origene	Cat no: TA150041
Mouse monoclonal anti-myc antibody	Sigma-Aldrich	Cat no: M4439
Anti-glyceraldehyde-3-phosphate dehydrogenase (GAPDH)	Santa Cruz Biotechnology	Cat no: sc-332233
Secondary antibody	Supplier	Cat. no/Ref. no
Mouse IgG-BP-HRP (horseradish peroxidase)	Santa Cruz Biotechnology	Cat no: sc- 516102

**Table 6. Chemicals and materials for SDS acrylamide gel**

Reagent	Supplier	Cat. no/Ref. no
30% Acrylamide/ Bis Solution 37.5:1	BIO-RAD	Cat: 1610158
Tris-HCl 2M pH= 8.8		Made in lab
SDS 20%	BDH Biochemical	Ref: 44215HN
N,N,N,N- tetramethylethylenediamine (Temed) approx. 99%	Sigma-Aldrich	Cat no: T9281
Ammonium Persulfate 10%	Sigma-Aldrich	Cat no: A3678
TX sample buffer (4x)	BIO-RAD	Cat no: 1610791
DL-Dithiothreitol, MW=154.25 g/mol	Sigma-Aldrich	Cat no: D9779
Magic marker XP protein standard	Invitrogen	Ref: P/N LC 5602

Precision plus protein standard (Dual color)	BIO-RAD	Cat no: 1610374
--	---------	-----------------

**Table 7: Materials used in Western blotting**

Materials	Supplier	Cat. no/Ref. no
Instant dried Skimmed Milk	TESCO	
Triton X-100	Sigma-Aldrich	Cat no: T8787
Tween 20	Sigma-Aldrich	Cat: P 2287
Trizma Base	Sigma-Aldrich	Cat no: T1503
Pierce™ ECL western blotting substrate	Thermo Scientific	Ref: 32106

**Table 8: Materials used for gel chromatography analysis.**

Materials	Supplier	Cat. no/Ref. no
Sephadex G-25 Superfine	GE Healthcare.	Cat no: 17-0031-01
polypropylene cap.Simport™Scientific 6.5mL HDPE Snaptwist™ Scintillation Vials		
1 M NaCl	Sigma-Aldrich	Cat no: 31434
Optiphase Hisafe 3 scintillation cocktail	PerkinElmer	1200.437

**Table 9. cDNA preparing reagent and PCR reagents**

Reagent	Supplier	Cat. no/Ref. no
5x iScript Reaction Mix	BIO-RAD	Cat no: 1708891
iScript Reverse transcriptase	BIO-RAD	Cat no: 1708891
Sybr green supermix	BIORAD	Cat no: 1708882

**Table 10: Primers used in RT-PCR**

Primer	Sequence forward primer (5' - 3')	Sequence reverse primer (5' - 3')
EXT1 Primer pair 1	CAACTGGCCAACACTGTGAGGA	CGGGAAGTCTGTCCCATCATT
EXT2 Primer pair 1	TGGGATCGAGGAACAAATCACC	TGCCGGTAAGTCCAGGTAGAA
Beta Actin	GGC TGT ATT CCC CTC CAT CG	CCA GTT GGT AAC AAT GCC ATG T
S-26	AAT GTG CAG CCC ATT CGC TG	CTT CCG TCC TTA CAA AAC GG
EXT1 Primer pair 2	GCT CTT GTC TCG CCC TTT TGT	TGG TGC AAG CCA TTC CTA CC

EXT2 Primer pair 2	AAG CAC CAG GTC TTC GAT TAC C	GAA GTA CGC TTC CCA GAA CCA
hHPRT	CTT CCT CCT CCT CCT GAG CAG	TCG AGC AAG ACG TTC AGT CC
POLR2F	CAC CCC CCA GTC TTC ATA GC	CCC GAA AGA TCC CCA TCA T

**Table 11: Materials used in immunofluorescence**

Name	Supplier	Cat. no/Ref. no
Collagen type I	Advance Bio Matrix	Cat no: 5005
Primary antibody: Mouse monoclonal turboGFP antibody	Origene	TA150041
Secondary antibody: Alexa Fluor 488-conjugated AffiniPure Goat anti mouse IgG	Jackson ImmunoResearch Laboratories	Cat no: 115-545-146
4% PFA Paraformaldehyde (PFA)	Thermo Scientific	Ref: 28908
4',6-diamidino-2-phenylindole (DAPI)	Invitrogen	Ref: P36935

**Table 12: Materials used for metabolic labeling of cells**

Name	Supplier	Cat. no/Ref. no
DEAE-Sephacel	Amersham Biosciences	Cat no: 17-0500-01
PD 10 columns	GE Healthcare	Cat no: 17-0851-01
[ <sup>3</sup> H]Glucosamine-HCl	PerkinElmer	Cat.no: NET190A
Heparin		
AgNO <sub>3</sub>	Sigma-Aldrich	Cat.no: 7761-88-8
Superose 6	GE Healthcare	Cat.no: 17-5172-01
Chondroitinase ABC	Sigma-Aldrich	Cat.no: C2905-10UN

## 5 METHODS

### 5.1 Cell culture

To ensure sterile conditions and prevent contamination all cell culture work was performed in a laminar flow bench with HEPA filter, and all equipment and work areas were disinfected with 70 % ethanol before starting work. The cells were grown in monolayer in culture flasks in Dulbecco's Modified Eagle Medium (DMEM), supplemented with 10% (v/v) fetal bovine serum 1% antibiotic-antimycotic solution (10,000 units/ml penicillin, 10,000 µg/ml streptomycin and 25 µg/ml Gibco Amphotericin B) and 1% L-glutamine at 37 °C, in a standard 5% CO<sub>2</sub> cell culture incubator.

### 5.2 Cell splitting

Cell splitting, also called cell passaging, is an essential process for the growth and multiplication of cells. Once the available substrate surface is covered by cells (a confluent culture), growth slows down and eventually ceases. To ensure that the cells stay alive, the cells were split, diluted and transferred to a new culture flask. The medium in the cell culture flask was removed and the cells were washed three times with 5 ml sterile Dulbecco's phosphate buffered saline (PBS) at room temperature. To detach the cells from the flask, 1 ml of trypsin was added and cells incubated 3 to 4 minutes at 37 °C. When the cells rounded up and detached, trypsin was inhibited by the addition of 6 ml of the pre-warmed cell culture medium. The detached cells were transferred to new cell culture dishes. Due to fast growing nature of B16F10 mouse melanoma cells, they were split at a ratio of 1:10 every day to prevent over-confluency.

### 5.3 Cell Freezing

Freezing down of cells is an important factor to maintain the cell line at a low passage number, without contamination and genetic drift. Continuous growth of cells increases the passage number of the cell line increases the risk of a cellular alteration and contamination. Cells at 80%-90% confluency were trypsinized, resuspended in culture medium and centrifuged at 1000 rpm for 5 min. The supernatant was discarded, and the cell pellet was resuspended in cold freezing medium, containing 10% DMSO, 20% FBS and 70% culture medium. The cell suspension was then aliquoted into Cryovial tubes and stored in a Cool Cell box (Biocision) at -85°C for a few days, and then transferred to tank of liquid nitrogen for long-term storage.

#### 5.4 Cell transfection

Full-length C-terminal Turbo GFP-tagged EXT2 or full-length C-terminal Myc-DDK-tagged EXT1 in the PCMV-6-AC-GFP plasmid vector were transiently transfected into mouse B16-F12 and human MV3 melanoma cell lines. Cells were cultured to 80 % confluent in T75 cell culture flasks. After trypsinization, cells were resuspended in 10 ml of culture medium. Next, cells were gently seeded in pairs of different concentrations in 6 cm petri dishes and incubated at 37°C overnight. The following day, the dishes with approximately 50-60% cell confluency were selected for transfection. Cells were transiently transfected using Lipofectamine 2000 (Invitrogen). Briefly, cells were transfected with 1:3 ratio of plasmid ( $\mu\text{g}$ ) and Lipofectamine 2000 ( $\mu\text{l}$ ). Plasmid DNA-Lipofectamine complexes were added dropwise to the cells and cells incubated at 37°C. After 5 hours, 3 ml of cell culture medium containing 20% FBS was added to the cells and the cells were further incubated for 16-18 hours. Then, cells were extracted for transferase assay, protein analysis and total RNA isolation. Cells treated with only lipofectamine were used as controls.

#### 5.5 Protein expression analysis

The culture dish was washed twice with warm PBS. Thereafter, 0.25 ml of cold PBS was added, and cells were detached from the surface using a cell scraper. The total lysate was collected and placed on ice. Samples were centrifuged at 1300 rpm for 10 min at 4 °C. The supernatant was discarded. The pellet was resuspended in 80  $\mu\text{l}$  of lysis buffer containing protease inhibitor cocktail and incubated on a rotating shaker for 30 min at 4 °C. The sample was then centrifuged for 30 min at 13000 rpm at 4 °C. The supernatant was collected, and an aliquot immediately used for transferase assay and the remaining lysate for Western blot and BCA protein analysis.

#### 5.6 Glycosyltransferase assays

To investigate if the expressed EXT1 and EXT2 were able to transfer a single sugar residue to an acceptor oligosaccharide (Fig. 8), cell lysates were centrifuged, and the supernatants immediately used for transferase assays. Lysates, corresponding to approx. 10-40  $\mu\text{g}$  protein were incubated over-night at 37°C with 0.125  $\mu\text{Ci}$  of  $^{14}\text{C}$ - or  $^3\text{H}$ -labeled UDP-sugars (62.5  $\mu\text{Ci}/\mu\text{mol}$ ; prepared by mixing radiolabeled and unlabeled UDP sugars) and 45  $\mu\text{g}$  of oligosaccharide acceptor in a total volume of 25  $\mu\text{l}$  of 10 mM  $\text{MgCl}_2$ , 60 mM  $\text{NaCl}$ , 20 mM  $\text{MnCl}_2$ , 5 mM  $\text{CaCl}_2$  and 20 mM HEPES,

pH 7.4 (final concentrations). To measure GlcA-transferase activity,  $^{14}\text{C}$ -labeled UDP-GlcA and  $[\text{GlcNAc-GlcA}]_n$ - oligosaccharide acceptors were used. To measure GlcNAc-transferase activity,  $^3\text{H}$ -labeled UDP-GlcNAc and GlcA- $[\text{GlcNAc-GlcA}]_n$  acceptors were used (Fig. 8). The reaction products were analyzed by gel chromatography and quantified by scintillation counting.

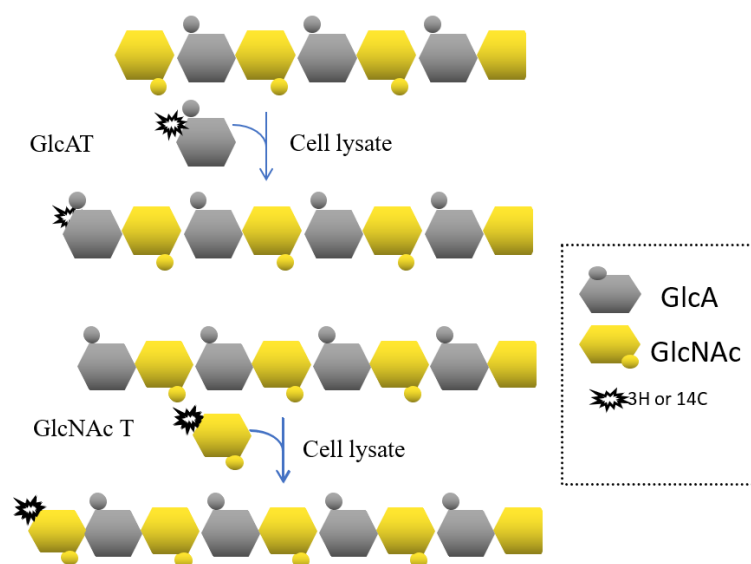


**Fig. 8: Schematic figure showing the principal of single sugar transferase assays.** Cell lysate were incubated with polysaccharide acceptors ( $\text{GlcA-}[\text{GlcNAc-GlcA}]_n$  or  $[\text{GlcNAc-GlcA}]_n$  and radiolabeled UDP-sugar. Active proteins transfer a single sugar unit to the acceptor molecule resembling the unmodified HS chain. The figure was provided by Prof. M.Kusche-Gullberg.

## 5.7 Western blot analysis.

Cell lysates (described in protein extraction section) were used for BCA protein assay, SDS-PAGE and Western blot analysis.

### 5.7.1 BCA protein assay

Total protein concentration of whole cell lysate was measured using Pierce™ BCA Protein Assay Kit following the manufacturer's protocol. Samples were prepared at 1:10 dilution using Milli-Q water. Serial dilutions of BSA (0, 25, 125, 250, 500, 750 and 1000  $\mu\text{g/ml}$ ) measured in duplicates were used to generate a standard curve. The concentration of samples was measured at  $22.7^\circ\text{C}$  at 562 nm absorbance using a Spectra Max Plus 384 Microplate Spectrophotometer.

### 5.7.2 SDS PAGE electrophoresis

SDS PAGE (sodium dodecyl sulfate–polyacrylamide gel electrophoresis) is used for separation of proteins by molecular weight in response to a supplied electric field. 50 µg of each protein samples were mixed with 10 µl of TX sample buffer (4x) containing 200 mM DL-Dithiothreitol (DTT) and the total sample volume was made up to 40 µl using sterile distilled water. The samples were separated on a 10% SDS-PAGE (using Mini-Protein short glass plates of 1.5 mm thickness, BioRad) for approximately 75 minutes at 125V. Magic marker (Invitrogen) and Precision plus protein standard (Dual color) were used as molecular weight markers.

Transfer of the proteins to an iBlot Gel transfer nitrocellulose membrane (Invitrogen) was done using an iBlot 2 Gel Transfer Device (semi-dry transfer device). After transfer, the membranes were stained with 0.1% (w/v) Ponceau in 5% acetic acid for approx. 5 minutes. Ponceau red is a red solution that reversibly binds to proteins. This gives information about the efficiency of the transfer. The membrane was then de-stained with 1x-TBS/T (1x TBS+ 0.1% Tween 20). To prevent unspecific binding of the antibodies to the membrane the membrane was blocked in 5% skimmed milk dissolved in TBS-T at room temperature for 1 hour. Thereafter, the blot was incubated at 4°C with the primary antibody overnight on a rocking table. For detection of tGFP-EXT2 a primary mouse monoclonal turbo-GFP antibody (1:200 dilution, Origene) was used. For detection of myc-EXT1 a primary mouse myc antibody (1:500 dilution, Sigma-Aldrich) was used. GAPDH mouse monoclonal antibody (1:2000, Santa Cruz) was used as an internal loading control. Next, the membrane was washed 3 x 10 min using 1 x TBS-T to wash away unbound antibodies. The blot was then incubated with the secondary antibody Mouse IgG- BP-HRP (Horseradish peroxidase, 1:5000) for 1 hour at 37 °C. Finally, the membrane was washed 3 x 10 min in 1X TBS-T and the bands detected using ECL Western Blot Detection kit (Pierce). The kit detects the HRP-labeled secondary antibodies bound to primary antibodies, resulting the formation of a fluorescent product which is visualized using Gel Doc Imaging system (BIO-RAD). The bands were quantified using the ChemiDOC™ XRS+ with image lab™ Software.

## 5.8 Gel Chromatography

Gel chromatography is a technique to separate molecules according to their difference in molecular weight or size. The molecules in the sample are pumped through columns containing such microporous gels. Larger molecules elute first and is followed by smaller molecules.

### 5.8.1 Gel column preparation

The column was prepared using Sephadex G-25 Superfine gel filtration resin. 15g of Sephadex superfine was mixed with 200 ml of distilled and the resin was allowed to swell overnight to form a gel. The following day, the gel was pipetted into the column without getting any air bubbles.

### 5.8.2 Sephadex G-25 gel chromatography

To separate oligosaccharide acceptor molecules that have incorporated a radiolabeled sugar (Fig. 9) from unincorporated radiolabeled UDP-sugars, the assay mix was loaded onto Sephadex G-25 gel chromatography column run in 1 M NaCl. Loading of samples were followed by rinsing the tube with 1 M NaCl to ensure that the entire sample was loaded into the gel. The eluates were collected in Scintillation Vials for 4 min/vial. 3 ml of Optiphase Hisafe 3 scintillation cocktail was added in each tube. Radioactivity was detected by the scintillation counting by Liquid Scintillation Analyzer supplied (Packard).

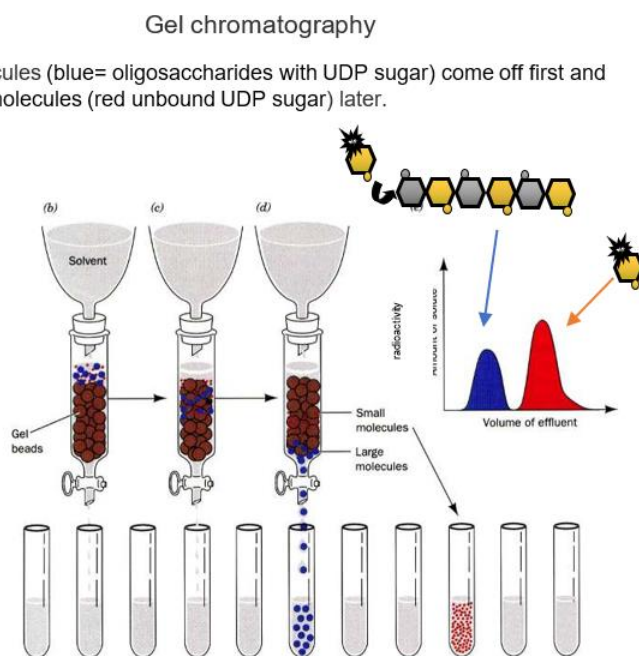




**Fig. 9: Figure shows the principle of gel chromatography.** Blue indicates oligosaccharide acceptor molecules that have incorporated a radiolabeled sugar and red, free, unincorporated, labeled UDP-sugars. Modified from <https://www3.nd.edu/~aseriann/CHAP6B.html/sld002.htm>

## 5.9 Gene expression analysis by RT-PCR

### 5.9.1 RNA extraction

RNA was extracted from ~80-90% confluent cells grown in cell culture petri dishes with a surface area of 25 cm<sup>2</sup>. The RNeasy Mini kit (Qiagen) was used to isolate RNA, following the protocol of the manufacturer. The total amount and purity of RNA was determined using NanoDrop 2000 Spectrophotometer (Thermo Scientific).

### 5.9.2 cDNA synthesis

cDNA was synthesized using iScript™ cDNA synthesis Kit (BioRad) used for reverse transcription of aliquots of 1 µg RNA to cDNA, following the manufacturers protocol. Briefly, 4 µl of 5x- iScript reaction buffer mix and 1µl of iScript reverse transcriptase were together added to the purified RNA samples, and the reaction mixture was incubated in the Thermal cycler to synthesize complementary DNA strands. The following reaction conditions were used: primer annealing at 25°C for 5 min, reverse transcription of RNA at 46°C for 20 min, enzyme inactivation at 95°C for 5 min and optional step- hold at 4°C. The synthesized cDNA was diluted at 1:9 ratio using Milli-Q water.

### 5.9.3 Quantitative real Time-Polymerase chain reaction (RT-PCR)

Quantitative-real Time-Polymerase chain reaction (RT-PCR) is used to analyze the degree of gene expression by determining the amount of amplified sample during each cycle, in real time, with forward and reverse primers of the target gene. Briefly, 6 µl iQSYBR Green supermix (Bio-Rad) was mixed with 0.5µl forward primer and 0.5 µl reverse primers (for list of primers see Table 11), and 5 µl of cDNA sample. The reaction mixture of each sample loaded in triplicates in a 384-well plate. The plate was covered and centrifuged 2 min at 2000 rpm and run on LightCycler® 480 system machine (Roche). The expression level of the EXT mRNA was normalized to that of the reference gene mRNA level. The relative expression levels were calculated using the  $2^{-\Delta\Delta CT}$  method (Livak & Schmittgen, 2001).

## 5.10 Immunofluorescence staining

Immunofluorescence staining of transiently transfected cells was done to see the transfection efficiency of EXT1KO and WT cells transfected with tGFP-tagged EXT2 DNA. The transfected cells were stained with an anti-tGFP antibody and observed under fluorescence microscope.

### 5.10.1 *Cell plate preparation*

Cover slips were prepared by washing with soap for 10 min followed by rinsing with water and 70% ethanol. After drying the coverslips were inserted into a 12-well plate, coated with collagen type I (100 µg/ml) and incubated for 1 hour at 37°C and then washed 3 x 5 min with PBS.

### 5.10.2 *Cell staining*

Cells in suspension were counted using Casy Modell TT, SCHÄRFE System. EXT1KO and WT cells were seeded on the prepared cover slips, 20 000 cells in each well. After 24 hours the cells were transiently transfected with the tGFP tagged EXT2 DNA plasmid. Control cells were treated with only Lipofectamine 2000. After 5 hours, 3 ml of 20% FBS medium was added into each well and the plate incubated 16-18 hours more. After 24 hours of transfection cell were stained. To stain for tGFP, cells were washed three times in PBS, fixed with freshly prepared 4% PFA (Paraformaldehyde), washed three times with PBS, permeabilized in 0.1% TX-100 for 15 min at room temperature and blocked with 10% bovine serum albumin in PBS for 1 hour. Cells were then incubated with the anti tGFP monoclonal antibody (1:200) at room temperature for 45 min. Thereafter, cells were washed 3 x for 10 min at room temperature using 0.1% PBS-Tween-20 and incubated with the secondary antibody Alexa fluor goat anti-mouse 488 (1:400). Cells incubated with only the secondary antibody was used as controls. After addition of the secondary antibody the plate was kept in dark for 1 hour at room temperature and then washed 3 x 10 min with PBS containing 0.1% Tween-20. Cells were mounted using ProLong Gold antifade reagent with DAPI (Invitrogen) and were incubated overnight. The following day, slides were observed under Zeiss AxioScope microscope equipped with optics for observing fluorescence and captured using a digital AxioCam MRm camera in a dark room at 40x magnification.

### 5.11 Metabolic labeling with $^3\text{H}$ -glucosamine and analysis of heparan sulfate structure

This experiment was done to rescue HS from knock-out cells by reintroducing of corresponding EXTs. B16F10 mouse melanoma EXT1KO cell was transfected with myc-tagged EXT1 plasmid DNA and EXT2 KO cell was transfected with tGFP-tagged EXT2 plasmid DNA. Cells were transfected as described in “Cell transfection” section.

#### 5.11.1 $^3\text{H}$ -glucosamine metabolic labeling

After 24 hours of transfection, cells were metabolically labeled by replacing the medium with 4 ml fresh medium (DMEM and 10 % FCS, without antibiotics), contain approximately 50  $\mu\text{Ci/ml}$   $^3\text{H}$  Glucosamine-HCl. After 24 hours the medium was removed and stored at  $-20^\circ\text{C}$ . Cells were washed with 2 x 5 ml PBS and then solubilized in 1 ml solubilization buffer (1%TX-100, 0.15 M NaCl, 50 mM Tris/HCl pH 7.4) for at 4 hours at  $4^\circ\text{C}$  on a rocking table. Cells were harvested using a cell scraper, transferred to an Eppendorf tube, and collected by centrifugation at 2000 rpm for 15 min at  $4^\circ\text{C}$ . The supernatant was transferred to a new tube and an aliquot used for protein determination using the BCA protein determination kit. The remaining supernatant was alkali treated to release GAGs from the protein.

#### 5.11.2 Alkali treatment to release O-linked oligo and polysaccharides from proteins

NaOH, in a final concentration of 0.5 M, was added to the supernatant to separate the GAG chains from the core protein. After overnight incubation at  $4^\circ\text{C}$ , the samples were neutralized with HCl. The pH was adjusted to approximately pH 8.0.

#### 5.11.3 Isolate free chains on DEAE-Sephacel

Diethylaminoethyl (DEAE)-Sephacel (Amersham Biosciences) is a positively charged ion-exchange resin that retains negatively charged molecules. Columns were made with 500 $\mu\text{l}$  DEAE-Sephacel equilibrated in 5 ml equilibration buffer (0.05 M Tris/HCl pH 8.0 or 7.5, 0.15 M NaCl, 0.1% TX-100). 2 mg heparin was added to the DEAE-Sephacel columns to prevent unspecific binding and excess heparin was eluted with 2 M NaCl. Then columns were equilibrated in equilibrated buffer. The samples were diluted to a final concentration of 0.15 M  $\text{Cl}^-$  in 0.02 M Tris/HCl pH 8.0 and added to the column. and the column was washed 10 times with 500  $\mu\text{l}$  portions of the equilibration buffer and the eluate collected in 10 Eppendorf tubes. Then column then washed 10 times with 500  $\mu\text{l}$  portions of 0.05 M acetate pH 4.0, 0.15 M NaCl, 0.1% TX-100.

Followed by a third washing step was carried out 10 times with 500  $\mu$ l portions of 0.05 M Tris/HCl pH 8.0 or 7.5. Finally, the GAG chains were eluted by stepwise elution with 10 times x 500  $\mu$ l portions of 2 M NaCl. Radioactivity was measured for each fraction. 5  $\mu$ l from each fraction, 3 ml of Optiphase Hisafe 3 scintillation cocktail was added and the radioactivity measured by a scintillation counter. Radioactive positive fractions in the 2 M NaCl eluate were pooled and desalted on PD-10 gel filtration columns.

#### 5.11.4 *Desalting using PD 10 Columns*

To separate GAG chains from unwanted salt, the samples were transferred to a PD10 column (GE Healthcare) which is a pre-packed Sephadex<sup>TM</sup> G-25 resin. The column was first washed with 30 ml H<sub>2</sub>O. Then 1 mg heparin was added to the column to prevent unspecific binding followed by washing with 50 ml H<sub>2</sub>O. Then the sample was added to the column and the flow through collected. The GAG chains were eluted with 12 x 0.5 ml H<sub>2</sub>O. Fractions of 0.5 ml were collected and 5  $\mu$ l from each eluted were analyzed for <sup>3</sup>H-radioactivity by scintillation counting. To analyze for salt (NaCl), 20  $\mu$ l of each fraction was transferred to a transparent Eppendorf tube. After addition of 0.1% AgNO<sub>3</sub>, salt will be visible as a white precipitate (AgCl<sub>2</sub>). Salt-free <sup>3</sup>H-positive fractions were pooled and quantified. The pooled samples were freeze dried and then resuspended in water to a volume of about 500  $\mu$ l in total. 60 000 DPM from each sample, was transferred into a 1.5ml tube, dried in a SpeedVac (Thermo Savant SPD1010 SpeedVAC) and resuspended in 200  $\mu$ l H<sub>2</sub>O.

#### 5.11.5 *Chondroitinase ABC digestion*

To remove CS from the purified samples, an aliquot (60 000 DPM) of the labeled samples was digested with chondroitinase ABC (Sigma) into disaccharides. Digestion was carried out overnight at 37°C in a buffer containing 100  $\mu$ g chondroitin sulfate, 50mM Tris-HCl pH 8.0, 30 mM Na-acetate, 0.1mg/ml bovine serum albumin and 0.2 units chondroitinase ABC. After overnight incubation, the sample was transferred to -20°C for 2 hours to inhibit the remaining enzyme activity. The sample was then centrifuged for 10 minutes at maximum speed and transferred to a clean Eppendorf tube. Next, 300  $\mu$ l 0.5 M NH<sub>4</sub>HCO<sub>3</sub> was added to the sample which was then centrifuged again to precipitate and remove any impurities. The samples were then analyzed using a Superose 6 HPLC gel filtration column.

#### 5.11.6 *Superose 6 HPLC gel filtration column*

Superose 6 is a HPLC gel filtration column (Amersham Biosciences) used for determining HS chain length. After addition of 300  $\mu$ l 0.5 M  $\text{NH}_4\text{HCO}_3$ , the samples were centrifuged to precipitate and remove any impurities before they were analyzed using a Superose 6 HPLC gel filtration column. The smaller fragments (CS disaccharides) are retained longer in the beads, whereas the larger fragments (HS chains) pass alongside the beads, thus exiting the column first. The samples were collected in 60 fractions of 500  $\mu$ l and the radioactivity measured by scintillation counting.

## 6 RESULTS

EXT1 and EXT2 protein have major role in HS chain elongation by adding GlcA and GlcNAc in an alternative manner to the growing HS chain. Previous results have shown that both EXT1 and EXT2 are necessary for chain elongation *in vivo*. In *in vitro* assays, EXT1 has readily detectable enzyme (glycosyltransferase) activities but, it has been difficult to determine the enzyme activities of the EXT2 protein. This thesis deals with the individual roles of EXT1 and EXT2 in HS chain elongation with special focus on the enzymatic activities of EXT2. EXT enzymatic activities were examined using mouse or human melanoma cells lacking EXT1 (EXT1 knock-out, EXT1KO) or EXT2 (EXT2KO). Previous analysis in the lab of M. Kusche-Gullberg have shown that both EXT1KO and EXT2KO cells completely lack HS. To observe the individual functions of EXT1 and EXT2 and to prevent contribution of endogenous proteins, EXT1KO cells and EXT2KO cells were transiently transfected with plasmids expressing full-length human TurboGFP (tGFP)-tagged EXT2 and full-length human C-terminal myc-DDK-tagged EXT1, respectively. For control, wild type (WT) cells were also transfected and analyzed for activity.

### 6.1 EXT1 deficient (EXT1KO) B16F10 mouse melanoma cells transfected with tGFP tagged EXT2 plasmid DNA

#### 6.1.1 *Protein expression analysis by Western blotting.*

Full-length tGFP-EXT2 was transiently transfected into WT (WT+ EXT2) and EXT1KO (EXT1 KO+EXT2) B16F10 mouse melanoma cells using Lipofectamine. WT cells and EXT1KO cells treated with only Lipofectamine were used as controls, WT control and EXT1KO control, respectively. The experiment was repeated four times and the level of overexpression analyzed by Western blotting (WB) of cell lysates using an antibody to tGFP (Fig. 10A) and the expressed proteins quantified relative to GAPDH (Fig. 10B). tGFP-tagged EXT2 has an apparent molecular weight of 108 kDa while the weight of GAPDH is 36 kDa. Comparisons of the expression levels of WT+ EXT2 with the expression of the EXT1 KO+EXT2 cells, showed that the relative values of expression of tGFP-EXT2 protein in EXT1 KO+EXT2 cells were much lower than in WT+ EXT2 cells.

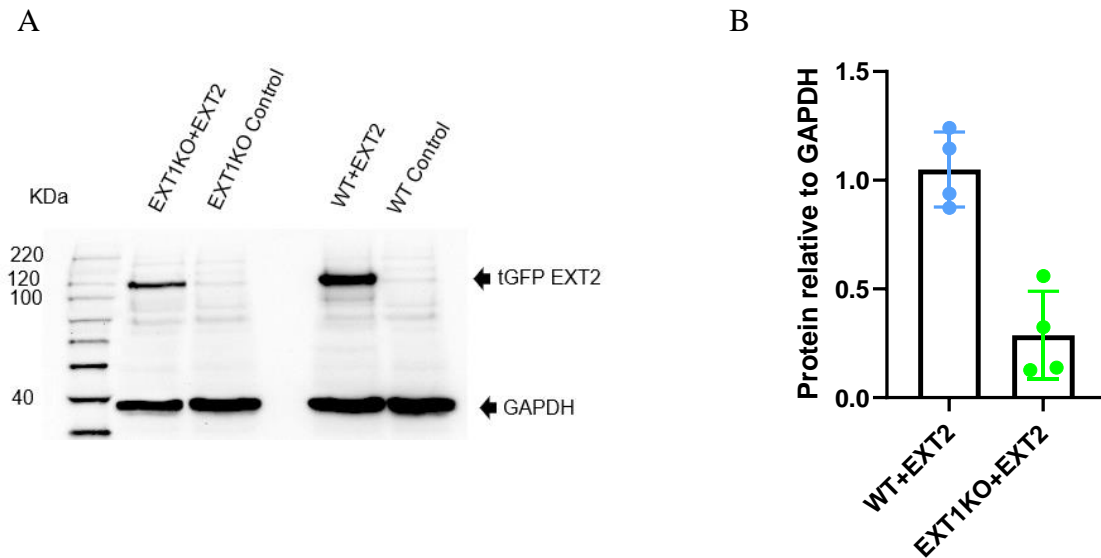


**Fig. 10: Western blot analysis (A) and quantification of the expressed tGFP-EXT2 protein (B).** (A) Cell extracts (50  $\mu$ g cellular protein /lane) from EXT2 transfected cells and transfection reagent only treated control cells were separated by SDS-PAGE and transferred to a polyvinylidene difluoride membrane (see “Methods”). The expressed proteins were detected with antibodies against tGFP (1:200) and GAPDH (1:2000) and visualized by chemiluminescence. Shown is one representative blot out of four separate experiments. The positions of molecular size standards (in kDa) are indicated. (B) The band intensity of detected proteins was quantified for all four experiments by Imagej software and presented in the bar graphs as relative to GAPDH.

### 6.1.2 *EXT2* mRNA expression levels in WT control, *EXT1KO* control, WT+ *EXT2* and *EXT1KO+EXT2* B16F10 mouse melanoma cells

To determine if the low amounts of expressed tGFP-EXT2 protein in EXT1KO+EXT2 cells were caused by an inhibition at the protein level (improper translation, folding or transport of the EXT2-protein) or a lower transfection efficiency, the relative amounts of EXT2 mRNA were determined by real-time PCR. RNA was extracted from the four different cell-types and cDNA was transcribed by reverse transcription and analyzed by PCR. The experiment was repeated three times. The expression level of EXT2 in EXT1KO control cells was similar to like WT control cell, showing that treatment with lipofectamine did not affect endogenous levels of EXT2. Similar to the results from protein analysis, EXT2 expression level was much higher in WT transfected cells than in EXT1KO cell transfected cells (Fig. 11), indicating that the transfection efficiency in EXT1KO cells was reduced compare to WT+EXT2 cells.

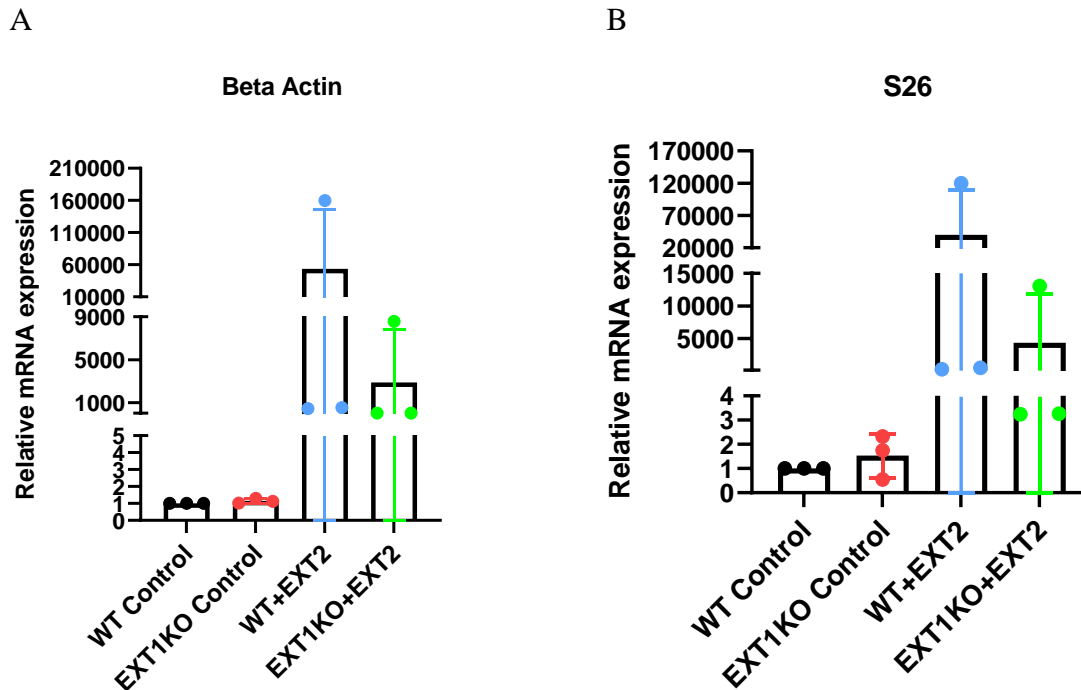


**Fig. 11: mRNA levels of EXT2 protein in transfected and non-transfected B16F10 mouse melanoma cells.** Cells were transiently transfected with tGFP-tagged EXT2 (WT+EXT2 and EXT1KO+EXT2) or treated with transfection reagent only (WT control and EXT1KO control) as described in “Methods”. 24 hours after transfection relative mRNA levels were determined by real time PCR and normalized to those of A) b-actin and B) S26. mRNA levels are expressed relative to the expression of the WT control that was set to 1. The error bars in A and B represent the mean from three independent transfections. Each measurement was performed in triplicate.

### 6.1.3 Glycosyltransferase activity in WT control, EXT1KO control and EXT1KO+EXT2 B16F10 mouse melanoma cells

To analyze the catalytic properties of EXT2 protein, two different *in vitro* transferase assays were employed, both of which quantify the transfer of single sugars to acceptor molecules. Oligosaccharides derived from *Escherichia coli* K5 capsular polysaccharide were used as acceptor molecules. The K5 polysaccharide has the same [GlcA-GlcNAc]<sub>n</sub> structure as nonsulfated HS. K5-oligosaccharides with non-reducing terminal GlcA or GlcNAc residues thus serve as acceptors in the GlcNAc- and GlcA-transferase reactions (see “Methods”, Fig. 8). The *in vitro* GlcA-transferase activity of EXT1KO+EXT2 cells were found to have increased approximately 20-fold as compared to EXT1KO cells (Fig. 12B). This result indicates that EXT2 protein has GlcA transferase activity.



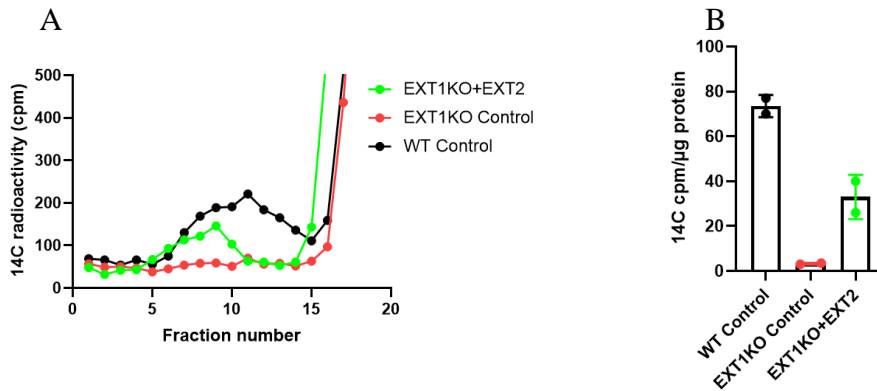


**Fig. 12: GlcA transferase activities in EXT2 transfected and non-transfected B16F10 mouse melanoma cells.**

Crude cell-lysates from cells, as indicated in the figures, were incubated with radiolabeled UDP-GlcA and unlabeled acceptor oligosaccharides with a nonreducing end GlcNAc and assayed for single-sugar transfer of GlcA to the acceptor. A) Gel chromatography of acceptor oligosaccharides with added GlcA (eluting around fractions 5-15). Material eluting after fraction 15 represent unincorporated labeled UDP-GlcA. B) Bar graphs show the incorporation of GlcA as radioactivity (cpm)/ mg protein. The figure is representative mean  $\pm$ SD from two independent experiments.

In contrast to the clear increase in GlcA-transferase activity there were no significant difference in GlcNAc-transfer between EXT1KO+EXT2 and EXT1KO cells. However, the KO cell showed some GlcNAc transferase activity (Fig. 13) which was unexpected. The GlcNAc transferase enzyme activity in EXT1KO calls may be due to the activity of EXTL3 as total cell lysate containing EXTL3 is known to transfer GlcNAc to K5 acceptors (Busse et al., 2007).

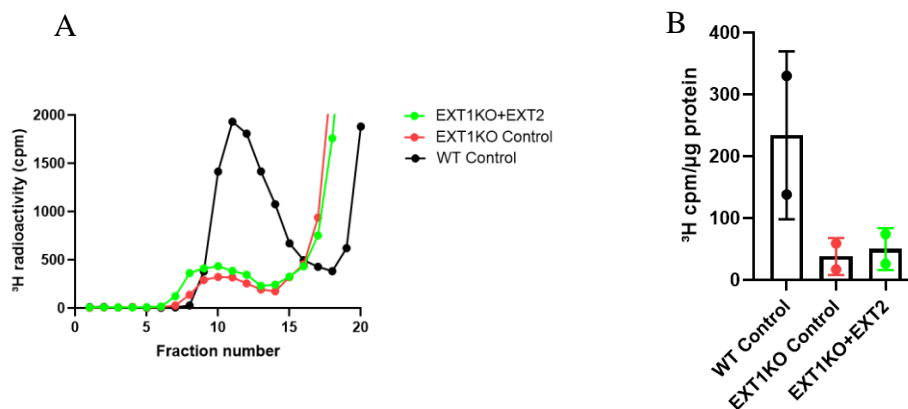


**Fig. 13: GlcNAc-transferase activities in EXT2 transfected and non-transfected B16F10 mouse melanoma cells.**

Crude cell-lysates from cells, as indicated in the figures, were incubated with radiolabeled UDP-GlcNAc and unlabeled acceptor oligosaccharides with a nonreducing end GlcA and assayed for single-sugar transfer of GlcNAc to the acceptor. A) Gel chromatography of acceptor oligosaccharides with added GlcNAc (eluting around fractions 5-15).

Material eluting after fraction 15 represent unincorporated labeled UDP-GlcNAc. B) Bar graphs show the incorporation of GlcNAc as radioactivity (cpm)/ mg protein. The figure is representative mean  $\pm$ SD two independent experiments.

#### 6.1.4 Immunofluorescence staining

To further investigate the low transfection efficiency of EXT1KO+EXT2 cells, EXT1KO+EXT2 and WT+EXT2 cells were stained using an antibody against the tGFP-tag. Transfected cells were fixed and stained with the primary antibody, mouse monoclonal anti turbo GFP (1:200) and the secondary antibody, Alexa Fluor goat anti-mouse 488 (1:400). Stained cells were mounted with DAPI to visualize nuclei. Immunofluorescence staining showed that the level of overexpression was relatively low in EXT1KO+EXT2 cells (Fig. 14). Only few EXT1KO+EXT2 cells expressed the tGFP-tagged EXT2.

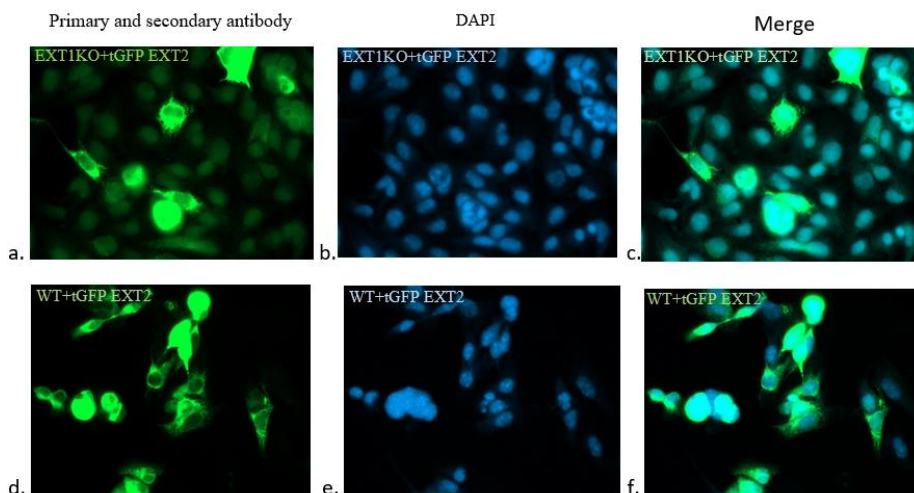


**Fig. 14: Immunofluorescence staining of EXT2 transfected cells.** EXT1KO and WT B16F10 cells were transiently transfected with the full-length tGFP-EXT2 expression plasmid. The transfected cells were fixed and stained for EXT2 (green) and the nuclei counterstained with 4',6'-diamino-2-phenylindole (DAPI, blue) as described in Methods section.

## 6.2 EXT1 deficient MV3 human cells transfected with tGFP tagged EXT2 plasmid DNA

The results after transfection of the B16F10 EXT1KO cells with tGFP tagged EXT2 plasmid DNA resulted in GlcA-transferase activity, indicating that EXT2 may be a GlcA-transferase. To further study this, similar experiments as with the B16F10 mouse melanoma cells lacking EXT1, were

done using another cell line, a human melanoma MV3 cell line. This experiment was done only one time.

### 6.2.1 Protein expression analysis by Western blotting

Full-length tGFP-EXT2 was transiently transfected into WT (WT+ EXT2) and EXT1KO (EXT1 KO+EXT2) MV3 mouse melanoma cells using Lipofectamine. WT cells and EXT1KO cells treated with the transfection reagent (Lipofectamine) alone were used as controls, WT control and EXT1KO control, respectively. The level of overexpression was analyzed by WB of cell lysates using an antibody to tGFP (Fig. 15A) and the expressed proteins quantified relative to GAPDH (Fig. 15B). Similar to transfection of tGFP-EXT2 into B16F10 EXT1KO cells, the protein expression levels in EXT1KO+EXT2 were lower than in WT+EXT2 cells. However, the difference in protein expression levels between EXT1KO+EXT2 and WT+EXT2 was not as large as in as in the experiment using mouse melanoma B16F10 cells (see Fig. 10B).

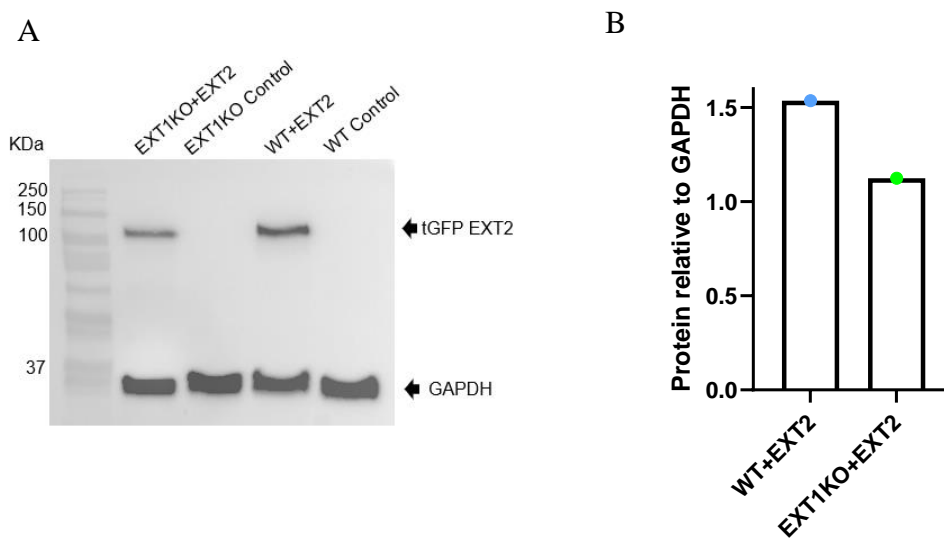


**Fig. 15: Western blot analysis (A) and quantification of the expressed tGFP-EXT2 protein (B).** (A) Cell extracts (35  $\mu$ g cellular protein /lane) from EXT2 transfected cells and transfection reagent only treated control cells were separated by SDS-PAGE and transferred to a polyvinylidene difluoride membrane (see “Methods”). The expressed proteins were detected with antibodies against tGFP (1:200) and GAPDH (1:2000) and visualized by chemiluminescence. The positions of molecular size standards (in kDa) are indicated. (B) The band intensity of detected proteins was quantified for one experiment by Imagej software and presented in the bar graphs as relative to GAPDH.

### 6.2.2 *EXT2* mRNA expression levels in WT control, *EXT1*KO control, WT+ *EXT2* and *EXT1*KO+*EXT2* MV3 human cells

The relative amounts of *EXT2* mRNA were determined by real-time PCR. RNA was extracted from the four different cell-types and cDNA was transcribed by reverse transcription and analyzed by PCR. The experiment was repeated two times. The expression levels of *EXT2* in *EXT1*KO control cells was similar to like WT control cell, again showing that treatment with Lipofectamine did not affect endogenous levels of *EXT2*. Similar to the results from protein analysis and experiments using the B16F10 tGFPEXT2 transfected cells, *EXT2* expression level was higher in WT transfected cells than in *EXT1*KO transfected cells (Fig. 16), again indicating that the transfection efficiency in *EXT1*KO cells was reduced compare to WT-cells.

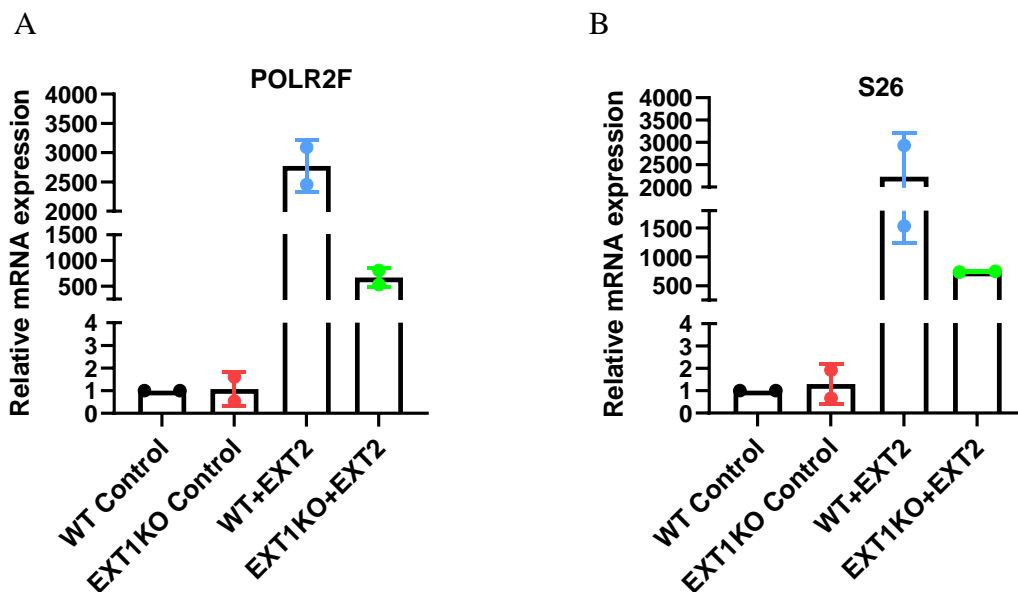


**Fig. 16: mRNA levels of *EXT2* protein in transfected and non-transfected MV3 human cells.** Cells were transiently transfected with tGFP-tagged *EXT2* (WT+ *EXT2* and *EXT1*KO +*EXT2*) or treated with transfection reagent only (WT control and *EXT1*KO control) as described in “Experimental”. 24 hours after transfection relative mRNA levels were determined by real time PCR and normalized to those of A) *POLR2F* and B) *S26*. mRNA levels are expressed relative to the expression of the WT control that was set to 1. The error bars in A and B represent the mean from two analysis of a single transfection. Each measurement was performed in triplicate.

### 6.2.3 Glycosyltransferase activity in WT control, EXT1KO control and EXT1 KO+EXT2 MV3 human cells

The catalytic properties of EXT2 protein were analyzed as in the experiments with B16F10 cells using two different *in vitro* transferase assays, both of which quantify the transfer of single sugars to acceptor molecules. In contrast to the experiment with B16F10 cells, the MV3 EXT1KO+EXT2 did not show any transfer of GlcA or GlcNAc (Fig. 17).

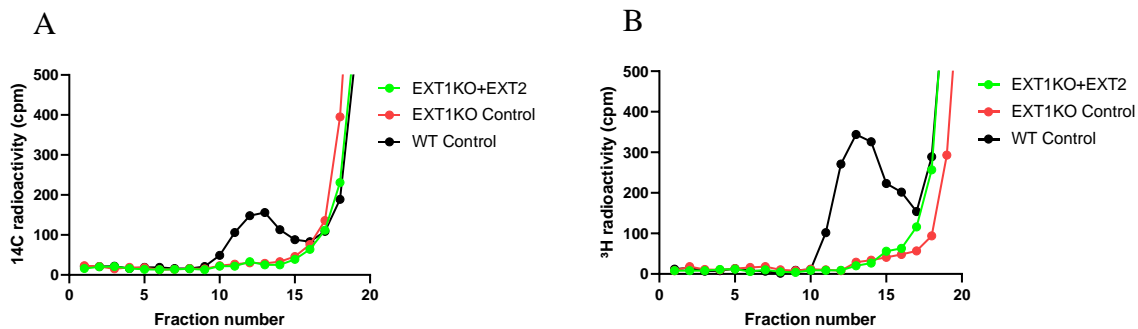


**Fig. 17: GlcA-transferase and GlcNAc activities in EXT2 transfected and non-transfected MV3 cells.** Crude cell-lysates from cells, as indicated in the figures, were incubated with either radiolabeled UDP-GlcA or UDP-GlcNAc along with the unlabeled acceptor oligosaccharides and assayed for single sugar transfer to oligosaccharides with a nonreducing end **A.** GlcNAc (GlcA transferase activity) or **B.** GlcA (GlcNAc transferase activity). Labeled acceptor molecules elute in fractions 10-15. Material eluting after fraction 15 represent unincorporated labeled UDP-sugars.

## 6.3 EXT2 deficient B16F10 mouse melanoma transfected with full-length human C-terminal myc-DDK-tagged EXT1 plasmid DNA

To study the enzyme activity of EXT1, cells lacking EXT2 were transfected with myc-DDK tagged EXT1 plasmid DNA and analyzed as in the experiments examining the enzyme activities of EXT2 using EXT1KO cells

### 6.3.1 Protein expression analysis by Western blotting.

Full-length myc-DDK tagged EXT1 was transiently transfected into WT (WT+ EXT1) and EXT2KO (EXT2 KO+EXT1) B16F10 mouse melanoma cells using Lipofectamine. WT cells and EXT2KO cells treated with the transfection reagent (Lipofectamine) alone were used as controls, WT control and EXT2KO control, respectively. The experiment was performed for single time and the level of overexpression analyzed by WB of cell lysates using an antibody to myc and

GAPDH (Fig. 18). myc-DDK tagged EXT1 has an apparent molecular weight of 87 kDa while the weight of GAPDH is 36 kDa.

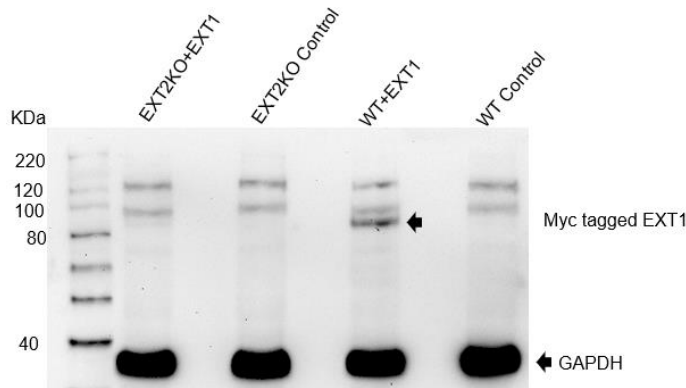


**Fig. 18: Western blot analysis.** Cell extracts (50  $\mu$ g cellular protein /lane) from EXT1 transfected cells and transfection reagent only treated control cells were separated by SDS-PAGE and transferred to a polyvinylidene difluoride membrane (see “Methods”). The expressed proteins were detected with antibodies against myc (1:500) and GAPDH (1:2000) and visualized by chemiluminescence. The positions of molecular size standards (in kDa) are indicated. Unspecific bands are observed in each lane. Arrow in 3<sup>rd</sup> lane indicates the myc tagged-EXT1 positive band in the WT+EXT1 sample.

### 6.3.2 *EXT1* mRNA expression levels in WT control, *EXT2KO* control, WT+ *EXT1* and *EXT2KO+EXT1* B16F10 mouse melanoma cells.

To determine the low amounts of expressed myc-DDK tagged EXT1 protein in WT+EXT1 cells and to analyze no transfected protein bands in EXT2KO+EXT1 cells, real-time PCR was performed. RNA was extracted from the four different cell-types and cDNA was transcribed by reverse transcription and analyzed by PCR. The experiment was done a single time. The expression level of EXT1 in EXT2KO+EXT1 cells was low, barely above the non-transfected EXT2KO control cells. The results from protein and mRNA analysis indicate poor transfection of EXT2KO+EXT1 cells (Fig. 19).

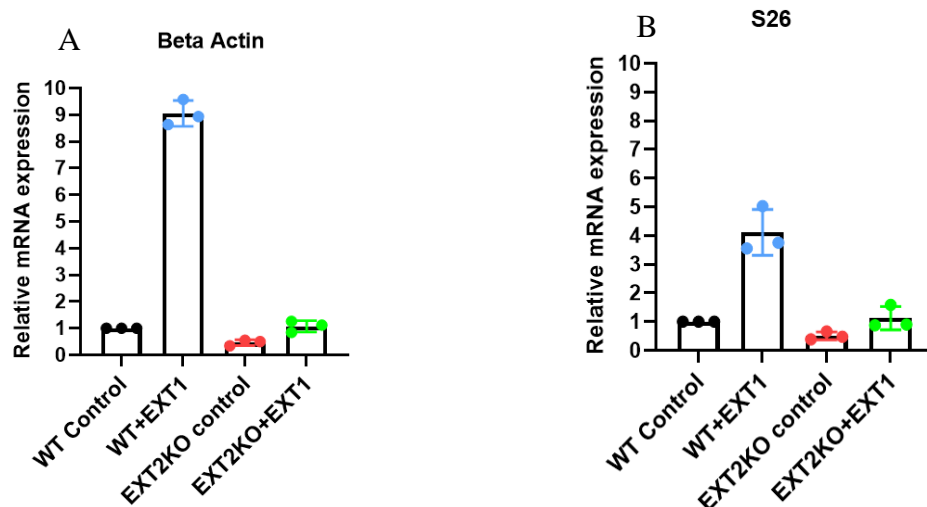


**Fig. 19: mRNA level of EXT1 protein in transfected and non-transfected B16F10 mouse melanoma cells.** Cells were transiently transfected with myc-DDK tagged EXT1 (WT+ EXT1 and EXT2KO +EXT1) or treated with transfection reagent only (WT control and EXT2KO control) as described in “Methods”. 24 hours after transfection relative mRNA levels were determined by real time PCR and normalized to those of A) Beta actin and B) S26. mRNA levels are expressed relative to the expression of the WT control that was set to 1. The bars in A and B represents real time PCR analysis of single transfection. Each measurement was performed in triplicate

### 6.3.3 Glycosyltransferase activity in WT control, EXT2KO control and EXT2 KO+EXT1 B16F10 mouse melanoma cells

The poor transfection results were also shown in the transferase assays (performed as described above). Transfected cells did not show any GlcA transferase activity and did not significant increase in GlcNAc transferase activity compared to EXT2KO control cells (Fig 20).

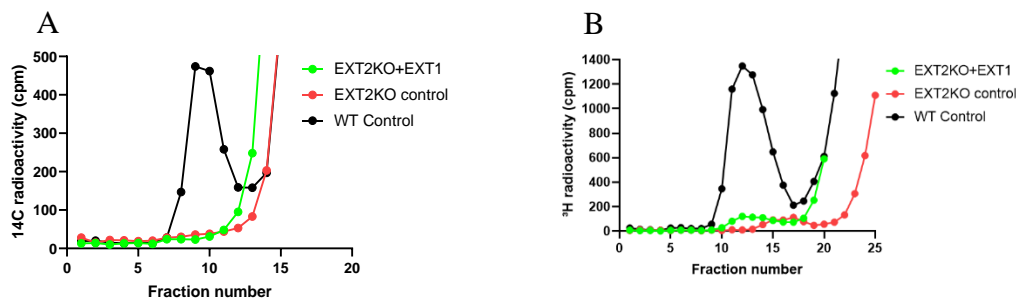


**Fig. 20: GlcA-transferase and GlcNAc activities in EXT1 transfected and non-transfected B16F10 mouse melanoma cells.** Crude cell-lysates from cells, as indicated in the figures, were incubated with either radiolabeled UDP-GlcA or UDP-GlcNAc along with the unlabeled acceptor oligosaccharides and assayed for single sugar transfer to oligosaccharides with a nonreducing end of A. GlcNAc (GlcA transferase activity) or B. GlcA (GlcNAc transferase activity). Labeled acceptor molecules elute in fractions 10-15. Material eluting around or after fraction 15 represent unincorporated labeled UDP-sugars.

## 7 DISCUSSION

By interaction with a multitude of different molecules, HS plays important roles in many processes during development and in the adult organism. The signaling pathways of many growth factors (such as FGF) are dependent on the presence of HS. It is therefore important to understand HS biosynthesis in order to understand its functions. EXT1 and EXT2 protein have essential roles in HS biosynthesis. *In vitro* experiments have showed that EXT1 protein has detectable glycosyltransferase activity, but that function of EXT2 in HS biosynthesis is puzzling. The main objective of this project was to study the enzymatic activity of EXT2 and EXT1, focusing on EXT2.

### *Expression and catalytic activities of EXT2 expressed in human and mouse EXT1KO cells*

EXT2 was transiently transfected into mouse melanoma B16F10 cells and human melanoma MV3 cells lacking EXT1. As controls EXT2 was also transfected into corresponding WT cells. Western blot analysis and RT-PCR revealed rather poor transfection of EXT2 into EXT1KO cells as compared to the transfection of WT cells (Figs 10, 11, 15, 16). The reduced transfection efficiency was confirmed for B16F10 EXT1KO cells by staining of transfected cells using an antibody against the tGFP-tag (Fig. 14). The transfection reagent, Lipofectamine, forms cationic liposome-DNA complexes, that bind to negatively charged molecules on the cell membrane. Then the complexes fuse with the membrane and DNA is internalized into the cytoplasm (FELGNER et al., 1995). The reason for the poor transfection efficiency of KO cells lacking HS is most probably due to lack of the negatively charged cell surface HS chains that are necessary for the attachment of cationic liposomes (Mounkes et al., 1998)(Letoha et al., 2013).

Transfection of EXT2 into mouse melanoma cells resulted in increased GlcA transferase activity (Fig. 12) but had no effect on GlcNAc transferase activity (Fig. 13). The EXT1KO cells had some but low GlcNAc transferase activity. This may be due to endogenous presence of EXTL3. EXTL3 has been shown to have GlcNAc-transferase activity but no GlcA transferase activity (Kim et al., 2001). In contrast, transfection of EXT2 into the human melanoma EXT1KO cells did not increase GlcA (or GlcNAc) transferase activity (Fig. 17). There is no clear explanation for why transfection of the human melanoma MV3 cell line gave a different result than transfection of the mouse melanoma cell line. In both cell lines CRISPR/Cas9 was used to deplete EXT1 using the same the target-specific CRISPR guide RNA (Dr. Christian Gorzelanny, personal communication). One



explanation can be that too little protein was used in the transferase assays. Only 15µg cellular protein were used whereas approx. 30 µg cellular protein was used in transferase assays using mouse melanoma cells.

In Kusche-Gullberg lab it has been verified that both the human and mouse KO cells completely lack HS chains. To confirm that the lack of HS in mouse EXT1KO and EXT2KO B16F10 cells were due to the deletion in EXT1 and EXT2 (caused by the CRISP-CAS9 treatment) an attempt was made to rescue these cells. To reintroduce EXT1 into EXT1KO cells and EXT2 into EXT2KO cells, the cells were transiently transfected with the myc-tagged EXT1 or tGFP-tagged EXT2, metabolically labeled with [<sup>3</sup>H]Glucosamine and the transfected cells analyzed for protein expression, mRNA expression and [<sup>3</sup>H]labeled HS chains (data not shown). The transfection did not work, no tagged protein bands were detected by WB. Metabolic labeling of cells confirmed that the KO cells did not synthesize HS (data not shown).

#### *Expression and catalytic activities of EXT1 expressed in mouse EXT2KO cells*

Myc-tagged EXT1 was transiently transfected into mouse melanoma B16F10 cells lacking EXT2 and, as a control, EXT1 was also transfected into WT B16F10 cells. The transfection efficiency was very low (Fig. 19) and only the transfected WT+EXT1 cells showed a weak band corresponding to the expressed myc-tagged EXT1 (Fig. 18). No GlcA transferase activity was observed in the EXT2KO control and EXT2KO+EXT1 cells. Some GlcNAc transferase activity was observed in both EXT1 transfected and KO control cells (Fig. 20). This may again be due to endogenous presence of EXTL3 in the cell lysates (Kim et al., 2001). It is difficult to draw any conclusion about the activity of EXT1 alone as the transfection appeared not to have worked. It is also possible that EXT1 protein cannot work properly in an EXT2 free background. In a study by (Busse & Kusche-Gullberg, 2003) it was shown that co-expression of EXT1 with EXT2 resulted in increased GlcA transferase activity compared to the activity of EXT1 alone. This indicates that EXT2 tends to enhance GlcA transferase activity but not GlcNAc transferase activity.

*What is the function of EXT2?*

Compared to EXT1, EXT2 has no clear glycosyltransferase activities but appears to have or at least promote GlcA transfer to the growing HS chain (Busse & Kusche-Gullberg, 2003). Clearly, EXT2 influences and modulates the enzymatic activity of EXT1. Silencing using siRNA (approx. 85-90% downregulation of mRNA expression) of EXT2 has the same effect on the HS chain length as silencing of EXT1. It results in short HS chains (Busse et al., 2007). Also, mice lacking either EXT1 or EXT2 has the same phenotype, they die before gastrulation and lack HS chains (Lin et al., 2000) (Stickens et al., 2005). Overexpression of EXT1 results on longer HS chains whereas overexpression of EXT2 has no effect on HS chain length (Busse et al., 2007). EXT2 is needed for HS chain elongation, maybe as a part of a EXT1/EXT2 elongating complex or as a transfer protein necessary for the transfer of EXT1 from the ER to the Golgi apparatus (Busse & Kusche-Gullberg, 2003) (McCormick et al., 2000)(Senay et al., 2000)

*Are the activities of EXT1 and EXT2 important for HS-protein interactions?*

One of the growth factors known to require HS for proper activation of its downstream signaling cascade, is FGF2. Fibroblasts with an EXT1 mutation that produce short HS chains with normal sulfation pattern show reduced proliferation rate, reduced FGF-2 signaling response and reduced ability to interact with collagen I (Österholm et al., 2009). These results show that the length of HS chains is a critical factor influencing HS-protein interactions.

## 8 CONCLUSION

EXT1 and EXT2 have previously been demonstrated to form a complex, which has been suggested to be the HS elongating unit. The EXT1/EXT2 complex formation seems to be necessary for the translocation of these proteins from the endoplasmic reticulum to the Golgi apparatus. Moreover, the transferase activities of the EXT1/2 complex have been shown to be enhanced in comparison to the activities of the EXT1 and EXT2 alone. We found that EXT2 alone have enhanced GlcA-transferase activity in the mouse melanoma cells but not in the human melanoma cells. The GlcA-transferase activity of EXT2 cannot be explained by the presence of the EXTL-proteins. The EXTL-proteins have GlcNAc-transferase activity, but none of the EXTL-proteins have GlcA-transferase activity.

Several questions remain:

**1. Is EXT2 a glycosyltransferase or needed for re-localization of EXT1 to the Golgi apparatus?**

To answer this question the experiments using EXT1KO cells need to be repeated and the glycosyltransferase activity of EXT2 needs to be determined after purification of EXT2 by immunoprecipitation after expression in EXT1KO cells.

**2. How does the EXT1/2 complex form?**

Complex formation can be studied by expressing epitope-tagged EXT1 expression construct lacking the short cytosolic part, the transmembrane region, the stem region, or the catalytic luminal region expressed in B16-F10 EXT1KO cells. Complex formation with EXT2 can be studied using Western blotting and enzyme assays.

## 9 REFERENCES

- Annaval, T., Wild, R., Créton, Y., Sadir, R., Vivès, R. R., & Lortat-Jacob, H. (2020). Heparan sulfate proteoglycans biosynthesis and post synthesis mechanisms combine few enzymes and few core proteins to generate extensive structural and functional diversity. In *Molecules* (Vol. 25, Issue 18). MDPI AG. <https://doi.org/10.3390/molecules25184215>
- Bethea, H. N., Xu, D., Liu, J., & Pedersen, L. C. (2008). *Redirecting the substrate specificity of heparan sulfate 2-O-sulfotransferase by structurally guided mutagenesis* Data deposition: *The atomic coordinates and structure factors have been deposited in the Protein Data Bank, www.pdb.org (PDB ID code 3F5F)* (Vol. 17, Issue 48).
- Bishop, J. R., Schuksz, M., & Esko, J. D. (2007). Heparan sulphate proteoglycans fine-tune mammalian physiology. In *Nature* (Vol. 446, Issue 7139, pp. 1030–1037). Nature Publishing Group. <https://doi.org/10.1038/nature05817>
- Busse, M., Feta, A., Presto, J., Wilén, M., Grønning, M., Kjellén, L., & Kusche-Gullberg, M. (2007). *Contribution of EXT1, EXT2, and EXTL3 to Heparan Sulfate Chain Elongation* \*. <https://doi.org/10.1074/jbc.M703560200>
- Busse, M., & Kusche-Gullberg, M. (2003). *In Vitro Polymerization of Heparan Sulfate Backbone by the EXT Proteins* \*. <https://doi.org/10.1074/jbc.M308314200>
- Busse-Wicher, M., Wicher, K. B., & Kusche-Gullberg, M. (2014). The extostoin family: Proteins with many functions. In *Matrix Biology* (Vol. 35, pp. 25–33). Elsevier. <https://doi.org/10.1016/j.matbio.2013.10.001>
- Cagno, V., Tseligka, E. D., Jones, S. T., & Tapparel, C. (2019). Heparan sulfate proteoglycans and viral attachment: True receptors or adaptation bias? In *Viruses* (Vol. 11, Issue 7). MDPI AG. <https://doi.org/10.3390/v11070596>
- Chen, J., Duncan, M. B., Carrick, K., Pope, R. M., & Liu, J. (2003). Biosynthesis of 3-O-sulfated heparan sulfate: Unique substrate specificity of heparan sulfate 3-O-sulfotransferase isoform 5. *Glycobiology*, *13*(11), 785–794. <https://doi.org/10.1093/glycob/cwg101>
- Clausen, T. M., Sandoval, D. R., Spliid, C. B., Pihl, J., Perrett, H. R., Painter, C. D., Narayanan, A., Majowicz, S. A., Kwong, E. M., McVicar, R. N., Thacker, B. E., Glass, C. A., Yang, Z., Torres, J. L., Golden, G. J., Bartels, P. L., Porell, R. N., Garretson, A. F., Laubach, L., ... Esko, J. D. (2020). SARS-CoV-2 Infection Depends on Cellular Heparan Sulfate and ACE2. *Cell*, *183*(4), 1043-1057.e15. <https://doi.org/10.1016/j.cell.2020.09.033>
- Crijns, H., Vanheule, V., & Proost, P. (2020). Targeting Chemokine—Glycosaminoglycan Interactions to Inhibit Inflammation. In *Frontiers in Immunology* (Vol. 11, p. 483). Frontiers Media S.A. <https://doi.org/10.3389/fimmu.2020.00483>
- de Waard, P., Vliegthart, J. F. G., Harada, T., & Sugahara, K. (1992). Structural studies on sulfated oligosaccharides derived from the carbohydrate-protein linkage region of chondroitin 6-sulfate proteoglycans of shark cartilage. II. Seven compounds containing 2 or 3 sulfate residues. *Journal of Biological Chemistry*, *267*(9), 6036–6043. [https://doi.org/10.1016/s0021-9258\(18\)42658-0](https://doi.org/10.1016/s0021-9258(18)42658-0)
- FELGNER, P. L., TSAI, Y. J., SUKHU, L., WHEELER, C. J., MANTHORPE, M., MARSHALL, J., & CHENG, S. H. (1995). Improved Cationic Lipid Formulations for In Vivo Gene Therapy. *Annals of the New York Academy of Sciences*, *772*(1), 126–139. <https://doi.org/10.1111/j.1749-6632.1995.tb44738.x>

- Filipek-Górniok, B., Habicher, J., Ledin, J., & Kjellén, L. (2021). Heparan Sulfate Biosynthesis in Zebrafish. In *Journal of Histochemistry and Cytochemistry* (Vol. 69, Issue 1, pp. 49–60). SAGE Publications Ltd. <https://doi.org/10.1369/0022155420973980>
- Forsberg, E., & Kjellén, L. (2001). Heparan sulfate: lessons from knockout mice. *Journal of Clinical Investigation*, 108(2), 175–180. <https://doi.org/10.1172/jci13561>
- Gallagher, J. (2015). *Fell-Muir Lecture: Heparan sulphate and the art of cell regulation: a polymer chain conducts the protein orchestra* INTERNATIONAL JOURNAL OF EXPERIMENTAL PATHOLOGY. <https://doi.org/10.1111/iep.12135>
- Häcker, U., Nybakken, K., & Perrimon, N. (2005). Heparan sulphate proteoglycans: The sweet side of development. In *Nature Reviews Molecular Cell Biology* (Vol. 6, Issue 7, pp. 530–541). Nature Publishing Group. <https://doi.org/10.1038/nrm1681>
- Hull, E. E., Montgomery, M. R., & Leyva, K. J. (2017). Epigenetic regulation of the biosynthesis & enzymatic modification of heparan sulfate proteoglycans: Implications for tumorigenesis and cancer biomarkers. In *International Journal of Molecular Sciences* (Vol. 18, Issue 7). MDPI AG. <https://doi.org/10.3390/ijms18071361>
- Kallunki, P., & Tryggvason, K. (1992). Human Basement Membrane Heparan Sulfate Proteoglycan Core Protein : A 467-kD Protein Containing Multiple Domains Resembling Elements of the Low Density Lipoprotein Receptor, Laminin, Neural Cell Adhesion Molecules, and Epidermal Growth Factor. In *The Journal of Cell Biology* (Vol. 116, Issue 2). <http://rupress.org/jcb/article-pdf/116/2/559/1062443/559.pdf>
- Katta, K., Imran, T., Busse-Wicher, M., Grønning, M., Czajkowski, S., & Kusche-Gullberg, M. (2015). Reduced expression of EXTL2, a member of the exostosin (EXT) family of glycosyltransferases, in human embryonic kidney 293 cells results in longer heparan sulfate chains. *Journal of Biological Chemistry*, 290(21), 13168–13177. <https://doi.org/10.1074/jbc.M114.631754>
- Kim, B. T., Kitagawa, H., Tamura, J. I., Saito, T., Kusche-Gullberg, M., Lindahl, U., & Sugahara, K. (2001). Human tumor suppressor EXT gene family members EXTL1 and EXTL3 encode  $\alpha$ 1,4-N-acetylglucosaminyltransferases that likely are involved in heparan sulfate/heparin biosynthesis. *Proceedings of the National Academy of Sciences of the United States of America*, 98(13), 7176–7181. <https://doi.org/10.1073/pnas.131188498>
- Kolset, S. O., & Pejler, G. (2011). Cells Chameleon with Wide Impact on Immune Serglycin: A Structural and Functional. *J Immunol References*, 187, 4927–4933. <https://doi.org/10.4049/jimmunol.1100806>
- Kramer, K. L. (2010). Specific sides to multifaceted glycosaminoglycans are observed in embryonic development. In *Seminars in Cell and Developmental Biology* (Vol. 21, Issue 6, pp. 631–637). Elsevier Ltd. <https://doi.org/10.1016/j.semcd.2010.06.002>
- Kusche-Gullberg, M., & Kjellén, L. (2003). Sulfotransferases in glycosaminoglycan biosynthesis. In *Current Opinion in Structural Biology* (Vol. 13, Issue 5, pp. 605–611). Elsevier Ltd. <https://doi.org/10.1016/j.sbi.2003.08.002>
- Ledin, J., Staatz, W., Li, J. P., Götte, M., Selleck, S., Kjellén, L., & Spillmann, D. (2004). Heparan sulfate structure in mice with genetically modified heparan sulfate production. *Journal of Biological Chemistry*, 279(41), 42732–42741. <https://doi.org/10.1074/jbc.M405382200>
- Letoha, T., Kolozsi, C., Ékes, C., Keller-Pintér, A., Kusz, E., Szakonyi, G., Duda, E., & Szilák, L. (2013). Contribution of syndecans to lipoplex-mediated gene delivery. *European Journal of Pharmaceutical Sciences*, 49(4), 550–555. <https://doi.org/10.1016/j.ejps.2013.05.022>

- Li, J. P., & Kusche-Gullberg, M. (2016). Heparan Sulfate: Biosynthesis, Structure, and Function. In *International Review of Cell and Molecular Biology* (Vol. 325, pp. 215–273). Elsevier Inc. <https://doi.org/10.1016/bs.ircmb.2016.02.009>
- Lin, X., Wei, G., Shi, Z., Dryer, L., Esko, J. D., Wells, D. E., & Matzuk, M. M. (2000). Disruption of gastrulation and heparan sulfate biosynthesis in EXT1-deficient mice. *Developmental Biology*, 224(2), 299–311. <https://doi.org/10.1006/dbio.2000.9798>
- Lind, T., Tufaro, F., McCormick, C., Lindahl, U., & Lidholt, K. (1998). The putative tumor suppressors EXT1 and EXT2 are glycosyltransferases required for the biosynthesis of heparan sulfate. *Journal of Biological Chemistry*, 273(41), 26265–26268. <https://doi.org/10.1074/jbc.273.41.26265>
- Lindahl, U., & Kjellén, L. (2013). Pathophysiology of heparan sulphate: Many diseases, few drugs. In *Journal of Internal Medicine* (Vol. 273, Issue 6, pp. 555–571). J Intern Med. <https://doi.org/10.1111/joim.12061>
- Livak, K. J., & Schmittgen, T. D. (2001). Analysis of relative gene expression data using real-time quantitative PCR and the 2- $\Delta\Delta$ CT method. *Methods*, 25(4), 402–408. <https://doi.org/10.1006/meth.2001.1262>
- Marie, A., Jousheghany, F., & Monzavi-Karbassi, B. (2011). On the Role of Cell Surface Chondroitin Sulfates and Their Core Proteins in Breast Cancer Metastasis. In *Breast Cancer - Focusing Tumor Microenvironment, Stem cells and Metastasis*. InTech. <https://doi.org/10.5772/20432>
- Mccormick, C., Duncan, G., Goutsos, K. T., & Tufaro, F. (2000). The putative tumor suppressors EXT1 and EXT2 form a stable complex that accumulates in the Golgi apparatus and catalyzes the synthesis of heparan sulfate. In *PNAS* (Vol. 97, Issue 2). [www.pnas.org](http://www.pnas.org)
- McCormick, C., Duncan, G., Goutsos, K. T., & Tufaro, F. (2000). The putative tumor suppressors EXT1 and EXT2 form a stable complex that accumulates in the Golgi apparatus and catalyzes the synthesis of heparan sulfate. *Proceedings of the National Academy of Sciences of the United States of America*, 97(2), 668–673. <https://doi.org/10.1073/pnas.97.2.668>
- Mounkes, L. C., Zhong, W., Cipres-Palacin, G., Heath, T. D., & Debs, R. J. (1998). Proteoglycans mediate cationic liposome-DNA complex-based gene delivery in vitro and in vivo. *Journal of Biological Chemistry*, 273(40), 26164–26170. <https://doi.org/10.1074/jbc.273.40.26164>
- Mulloy, B., Lever, R., & Page, C. P. (2017). Mast cell glycosaminoglycans. In *Glycoconjugate Journal* (Vol. 34, Issue 3, pp. 351–361). Springer New York LLC. <https://doi.org/10.1007/s10719-016-9749-0>
- Nagai, N., & Kimata, K. (2014). Heparan-sulfate 6-O-sulfotransferase 1-3 (HS6ST1-3). In *Handbook of Glycosyltransferases and Related Genes, Second Edition* (Vol. 2, pp. 1067–1080). Springer Japan. [https://doi.org/10.1007/978-4-431-54240-7\\_68](https://doi.org/10.1007/978-4-431-54240-7_68)
- Noborn, F., Gomez Toledo, A., Green, A., Nasir, W., Sihlbom, C., Nilsson, J., & Larson, G. (2016). Site-specific identification of heparan and chondroitin sulfate glycosaminoglycans in hybrid proteoglycans. *Scientific Reports*, 6(1), 1–11. <https://doi.org/10.1038/srep34537>
- Österholm, C., Barczyk, M. M., Busse, M., Grønning, M., Reed, R. K., & Kusche-Gullberg, M. (2009). Mutation in the heparan sulfate biosynthesis enzyme EXT1 influences growth factor signaling and fibroblast interactions with the extracellular matrix. *Journal of Biological Chemistry*, 284(50), 34935–34943. <https://doi.org/10.1074/jbc.M109.005264>

- Pacifici, M. (2017). Hereditary Multiple Exostoses: New Insights into Pathogenesis, Clinical Complications, and Potential Treatments. In *Current Osteoporosis Reports* (Vol. 15, Issue 3, pp. 142–152). Current Medicine Group LLC 1. <https://doi.org/10.1007/s11914-017-0355-2>
- Presto, J., Thuveson, M., Carlsson, P., Busse, M., Wilén, M., Eriksson, I., Kusche-Gullberg, M., & Kjellén, L. (2008). Heparan sulfate biosynthesis enzymes EXT1 and EXT2 affect NDST1 expression and heparan sulfate sulfation. *Proceedings of the National Academy of Sciences of the United States of America*, *105*(12), 4751–4756. <https://doi.org/10.1073/pnas.0705807105>
- Prydz, K., & Dalen, K. T. (2000). Synthesis and sorting of proteoglycans. *Journal of Cell Science*, *113*(2), 193–205. <https://doi.org/10.1242/jcs.113.2.193>
- Prydz, Kristian. (2015). Determinants of Glycosaminoglycan (GAG) Structure. *Biomolecules*, *5*. <https://doi.org/10.3390/biom5032003>
- Qin, Y., Ke, J., Gu, X., Fang, J., Wang, W., Cong, Q., Li, J., Tan, J., Brunzelle, J. S., Zhang, C., Jiang, Y., Melcher, K., Li, J. P., Xu, H. E., & Ding, K. (2015). Structural and functional study of D-Glucuronyl C5-epimerase. *Journal of Biological Chemistry*, *290*(8), 4620–4630. <https://doi.org/10.1074/jbc.M114.602201>
- Rabenstein, D. L. (2002). Heparin and heparan sulfate: Structure and function. In *Natural Product Reports* (Vol. 19, Issue 3, pp. 312–331). The Royal Society of Chemistry. <https://doi.org/10.1039/b100916h>
- Senay, C., Lind, T., Muguruma, K., Tone, Y., Kitagawa, H., Sugahara, K., Lidholt, K., Lindahl, U., & Kusche-Gullberg, M. (2000). The EXT1/EXT2 tumor suppressors: Catalytic activities and role in heparan sulfate biosynthesis. *EMBO Reports*, *1*(3), 282–286. <https://doi.org/10.1093/embo-reports/kvd045>
- Stickens, D., Clines, G., Burbee, D., Ramos, P., Thomas, S., Hogue, D., Hecht, J. T., Lovett, M., & Evans, G. A. (1996). The EXT2 multiple exostoses gene defines a family of putative tumour suppressor genes. *Nature Genetics*, *14*(1), 25–32. <https://doi.org/10.1038/ng0996-25>
- Stickens, D., Zak, B. M., Rougler, N., Esko, J. D., & Werb, Z. (2005). Mice deficient in Ext2 lack heparan sulfate and develop exostoses. *Development*, *132*(22), 5055–5068. <https://doi.org/10.1242/dev.02088>
- Takahashi, I., Noguchi, N., Nata, K., Yamada, S., Kaneiwa, T., Mizumoto, S., Ikeda, T., Sugihara, K., Asano, M., Yoshikawa, T., Yamauchi, A., Shervani, N. J., Uruno, A., Kato, I., Unno, M., Sugahara, K., Takasawa, S., Okamoto, H., & Sugawara, A. (2009). Important role of heparan sulfate in postnatal islet growth and insulin secretion. *Biochemical and Biophysical Research Communications*, *383*(1), 113–118. <https://doi.org/10.1016/j.bbrc.2009.03.140>
- van den Born, J., Gunnarsson, K., Bakker, M. A. H., Kjellén, L., Kusche-Gullberg, M., Maccarana, M., Berden, J. H. M., & Lindahl, U. (1995). Presence of N-unsubstituted glucosamine units in native heparan sulfate revealed by a monoclonal antibody. *Journal of Biological Chemistry*, *270*(52), 31303–31309. <https://doi.org/10.1074/jbc.270.52.31303>
- Wen, J., Xiao, J., Rahdar, M., Choudhury, B. P., Cui, J., Taylor, G. S., Esko, J. D., & Dixon, J. E. (2014). Xylose phosphorylation functions as a molecular switch to regulate proteoglycan biosynthesis. *Proceedings of the National Academy of Sciences of the United States of America*, *111*(44), 15723–15728. <https://doi.org/10.1073/pnas.1417993111>
- Wise, C. A., Clines, G. A., Massa, H., Trask, B. J., & Lovett, M. (1997). Identification and localization of the gene for EXTL, a third member of the multiple exostoses gene family. *Genome Research*, *7*(1), 10–16. <https://doi.org/10.1101/gr.7.1.10>